

**KNICKPOINT RETREAT AND FLUVIAL INCISION FOLLOWING  
THE 1999 CHI-CHI EARTHQUAKE: DA-AN RIVER GORGE,  
TAIWAN**

A Thesis  
Presented to  
The Academic Faculty

by

Ming-Chu Chen

In Partial Fulfillment  
of the Requirements for the Degree  
Master of Science in the  
School of Earth and Atmospheric Sciences

Georgia Institute of Technology  
August, 2010

**KNICKPOINT RETREAT AND FLUVIAL INCISION FOLLOWING  
THE 1999 CHI-CHI EARTHQUAKE: DA-AN RIVER GORGE,  
TAIWAN**

Approved by:

Dr. Kurt Frankel, Advisor  
School of Earth and Atmospheric Sciences  
*Georgia Institute of Technology*

Dr. Josef Dufek  
School of Earth and Atmospheric Sciences  
*Georgia Institute of Technology*

Dr. Zhigang Peng  
School of Earth and Atmospheric Sciences  
*Georgia Institute of Technology*

Date Approved: July 06, 2010

## ACKNOWLEDGEMENTS

I gratefully thank my advisor, Kurt Frankel for overseeing the completion of my master's thesis. His guidance is a priceless gift I gained in my academic career. I am definitely indebted to them. Many thanks to the local collaborators, Jien-Cheng Lee and Yu-Chang Chan who have supported the field work of this project and provided insightful comments since the beginning. Meng-Long Hsieh bought the Da-An River site to my attention. I thank my thesis reading committee of Josef Dufek and Zhigang Peng for providing constructive reviews that helped improve the manuscript.

Several people played a decisive role in bringing this work to fruition. I would like to extend my sincere thanks to Rou-Fei Chen, for her technical help in using RTK GPS and imagery analysis software. I could not make eight DEMs in a month, an impossible mission, without her knowledge. Additionally, I cannot finish this work without mentioning Peng Chao, who assisted me in Matlab programming. Thanks also to Kristen L. Cook, Su-Hao Chang, Yung-Chun Liu, Ting-Chieh Lin, Su-Chen Chiu, Yun-Hsuan Chen, De-Yang Yeh, Chia-Che Tsao, Li-Wei Chen, Pei-Fang Ho, and Ming-Che Chen for assistance in the field. Special thanks to Yi-Chen Chen, who taught me how to change the page orientation for a specific page in Microsoft Word. Writing class instructors Vitoria Van Cappellen and Jane Chisholm and officemate Joe Estep revised the manuscript in the different stages of this work. Rick Allmendinger released his Steronet program online for plotting joint data.

Personally, I would like to express my appreciation for the support by my family. You always allow me to freely pursue my dream and stand by my side when I make

decisions. I am not able to finish my thesis without your involvement. I also thank Yi-Chun Lin, my lovely girlfriend for her inspiration and encouragement when things are not going smooth.

This work was supported by the U.S. National Science Foundation East Asia and Pacific Summer Institute program, the Geological Society of America, Sigma Xi Grants-in-Aid of Research, Georgia Institute of Technology, and Academia Sinica.

# TABLE OF CONTENTS

	Page
ACKNOWLEDGEMENTS	iii
LIST OF TABLES	vii
LIST OF FIGURES	viii
SUMMARY	ix
<u>CHAPTER</u>	
1 Introduction	1
2 Study Area	5
2.1 Da-An River	5
2.2 1999 Chi-Chi Earthquake	6
3 Methods	8
3.1 Digital Elevation Model (DEM) Analysis	8
3.2 Global Position System Channel Surveys	9
3.3 Precipitation and Discharge	14
3.4 Rock Strength and Joint Orientation	14
4 Results	19
4.1 Evolution of Longitudinal Profiles	19
4.2 Precipitation and Discharge	25
4.3 Bedrock Structure	25
4.3.1 Rock Strength	25
4.3.2 Joint Orientations	26
4.3.3 Bedding Dip	26
4.4 Knickpoint Migration Rates	27

5	Discussion	29
5.1	Tectonic- and Climate- Driven Bedrock Incision	29
5.2	Structural and Lithologic Controls on the Evolution of the Da-An River Gorge	32
5.3	Implications for River Response to Coseismic Uplift	35
6	Conclusion	40
APPENDIX A: Field Survey Methodology and Uncertainties		42
REFERENCES		44

## LIST OF TABLES

	Page
Table 1: Hydroclimatological data for major flooding events in western Taiwan, 1999-2009	17
Table 2: Amount of knickpoint migration during the wet season (May-October, 2005-2009) and average dip angles of the bedrock bedding planes in which knickpoint migrated	18

## LIST OF FIGURES

	Page
Figure 1: Map of the Da-An River study area in central Taiwan	3
Figure 2: Photographs of the Da-An River in 1998, 2000, 2003, and 2008	4
Figure 3: Aerial photograph-derived digital elevation models	10
Figure 4: Aerial photos used for analyzing spatial-temporal changes of the lower Da-An River segment	11
Figure 5: Evolution of the longitudinal profile of the Da-An River from 1993 to 2009	12
Figure 6: Monthly average precipitation and discharge for the period 1999 to 2008 along the lower Da-An River	15
Figure 7: Equal area stereonet contour plot of poles to 1214 measured joint planes in the Da-An River Gorge	16
Figure 8: Schematic diagram illustrating how the Da-An River knickpoint migrates through the Tungshih anticline	22
Figure 9: Photographs of the dramatic channel changes between April, 2008 and January, 2009	23
Figure 10: Reach morphology classification	24
Figure 11: Linear regressions on knickpoint migration rate as a function of bedding dip	27
Figure 12: Linear regressions on knickpoint migration rate as a function of the maximum daily precipitation, total precipitation, and maximum hourly precipitation	34
Figure 13: A schematic showing how a river responds to coseismic uplift	38



## SUMMARY

The lower Da-An River in western Taiwan was uplifted ~10 during the 1999 Mw 7.6 Chi-Chi earthquake, resulting in a 20- to 30-m-deep bedrock gorge. However, the amount of coseismic displacement along the channel bed does not fully explain the resulting bedrock channel incision. Using a series of aerial photographs, digital terrain models (DEM), and real-time kinematic global positioning system (RTK GPS) surveys, we characterized knickpoint retreat and fluvial incision in the Da-An River gorge. We also analyzed discharge and precipitation data and collected measurements of rock strength and joint plane orientations to understand the climatic, lithological, and structural influence on the evolution of the actively incising gorge. Two stages of fluvial incision and knickpoint migration are identified in the gorge following surface uplift during the Chi-Chi earthquake. From 1999 to 2004, 3 to 5 m of alluvium was removed from the channel bed, followed by 3 to 4 m of bedrock channel incision. The knickpoint generated immediately after the earthquake remained where the uplift occurred at this time. Since 2005, the channel bed has lowered rapidly with local incision rates as high as 15 m/yr. The average knickpoint migration rate over the period 2005 to 2009 was 238 m/yr; total upstream migration from the location of knickpoint formation was 1190 m. While tectonic uplift formed the knickpoint and set the stage for channel incision, climate played a critical role in accelerating the fluvial response to coseismic displacement. More than 20 m of bedrock channel incision and 1180 m knickpoint migration occurred during the post-2004 typhoon seasons (May-October). Based on repeat surveys of the Da-An River longitudinal profile and analysis of precipitation and discharge data, we suggest

that a discharge threshold of 1200 to 2600 m<sup>3</sup>/s is required to initiate upstream knickpoint migration. However, once the threshold is exceeded, bedding dip becomes the primary control on rates and patterns of knickpoint propagation. Rotation occurred in a hinge zone where the bedding dips change from horizontal to upstream-dipping, while replacement was observed in the strata dipping upstream. The highest knickpoint migration rates (> 300 m/yr) were recorded in flat-lying, horizontal strata (< 10°) where parallel retreat was the dominate process. Overall, the knickpoint propagation followed the process of replacement behavior, in which the height of knickpoint decreases while migrating upstream. Thus, while tectonic processes set the initial conditions for knickpoint propagation in the Da-An River, the response time of the fluvial system to this forcing is strongly dependent on climate and local structure.

# **CHAPTER 1**

## **INTRODUCTION**

River incision into bedrock mirrors the effects of climate, tectonics, and even humans by responding to the change of boundary conditions such as base level, discharge, and sediment supply, thereby controlling the pace and style by which landscapes evolve (e.g., Leopold and Maddock, 1953; Hack, 1960; Bull, 1979; Howard et al., 1994; Tinkler and Wohl, 1998). A growing body of literature focused on the fluvial response to long-term tectonic uplift (e.g., Merritts and Vincent, 1989; Lave and Avouac, 2001; Snyder et al., 2003; Clark et al., 2004; Pearce et al., 2004; Stock et al., 2004; Harkins et al., 2007; Kirby et al., 2007; Oskin and Burbank, 2007; Whittaker et al., 2007b, Yanites et al., 2010a,b), rapid climate change (e.g., Reusser et al., 2004; Crosby and Whipple, 2006; Pelletier, 2009), mass-wasting (Brummer and Montgomery, 2006; Ouimet et al., 2007), and volcanic eruptions (Whipple et al., 2000b; Gran and Montgomery, 2005). These studies typically highlight the adjustment in channel gradient, channel width, and knickpoint retreat as a response process of river networks to changes in boundary conditions in terms of field surveys (e.g., Duvall et al., 2004; Stock et al., 2005; Amos and Burbank, 2007; Craddock et al., 2007; Whittaker et al., 2007a; Johnson et al., 2009), analogue experiments (e.g., Gardner, 1983; Turowski et al., 2006; Finnegan et al., 2007; Frankel et al., 2007; Johnson and Whipple, 2007; Douglass and Schmeeckle, 2007; Parker et al., 2008a), and numerical models (e.g., Finnegan et al., 2005; Stark, 2006; Berlin and Anderson, 2007; Attal et al., 2008; Parker et al., 2008b; Wobus et al., 2008; Turowski et al., 2009). Yet, field observations have provided inconsistent results of temporal adjustments in channel morphology in comparison to numerical and analogue experiments (Turowski et al., 2009). Therefore, natural experiments that utilize field

surveys to test and help modify existing process-based incision rules are necessary (e.g., Whipple, 2004).

Most natural perturbations occur over geologic time scales and often originate with unknown initial conditions. Thus, the duration and magnitude of these changes can be difficult to characterize. In most cases, documenting temporal changes in the landscape is impossible because fluvial response times occur over 0.25 to 2.5 Myr (Whipple and Tucker, 1999, 2002; Whipple, 2001) or longer (Schildgen et al., 2010).

One of the best natural laboratories in the world to study bedrock incision processes triggered by coseismic uplift and exacerbated by seasonal precipitation and human activities is the Da-An River, which is the northernmost major river along the 1999 Mw 7.6 Chi-Chi earthquake rupture trace in western Taiwan (Fig. 1). The surface rupture and resulting uplift of the Chi-Chi earthquake, which cuts orthogonally across several major rivers in western Taiwan, provides an exceptional opportunity to study the interaction between active tectonics, climate, and fluvial processes. Since being coseismically uplifted ~10 m and during the 1999 Mw 7.6 Chi-Chi earthquake (Lee et al., 2005), the Da-An River has undergone tremendous change from a channel mantled with 3 to 5 m of alluvium (Fig. 2A) to a >20-m-deep bedrock gorge (Fig. 2D). Because the incision processes in the Da-An River are occurring over similar time scales to analogue experiments, but on a natural scale, we can document the spatio-temporal change in channel morphology and accurately quantify landscape response to tectonic activity.

In this study we survey the distance, duration, and magnitude of channel incision following coseismic uplift in the Da-An River related to the 1999 Chi-Chi earthquake. We document knickpoint retreat, enhanced bedrock incision, and temporal changes in the river longitudinal profile to determine how a channel responds to a tectonic pulse. In addition, we present hydrological and lithological data such as discharge, precipitation, rock strength, and joint orientation to evaluate the impact of climate and lithology on

incision processes in the Da-An River. These data have important implications for fluvial incision processes and landscape evolution.

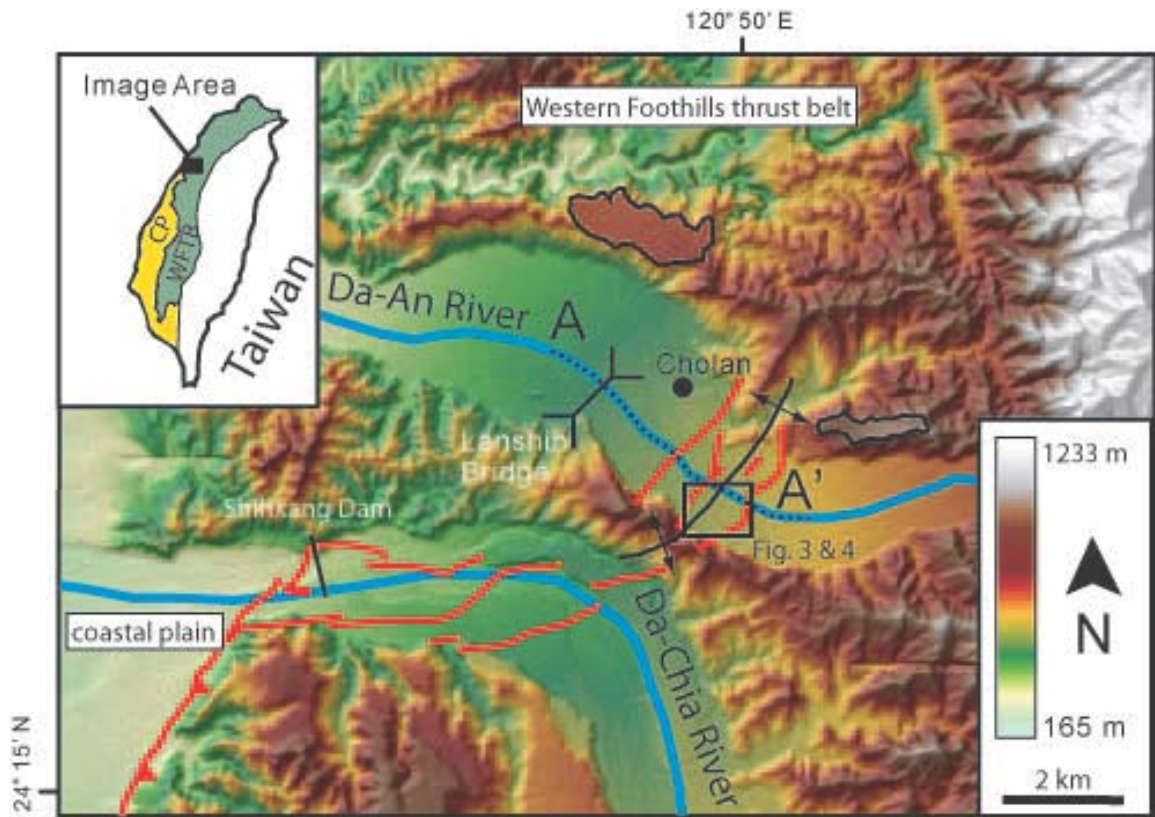


Figure 1. Map of the Da-An River study area in central Taiwan. Base is a 40-m-resolution digital elevation model (DEM) hillshade image (Central for Space and Remote Sensing Research, 1989). Red lines are the northern termination of the Chelungpu fault which ruptured in the 1999 Mw 7.6 Chi-Chi earthquake (Lee et al., 2002). Note that the surface rupture north of the Da-Chia River is characterized by wider zones of bending without an associated major fault cutting the land surface (Chen et al., 2007). Teeth indicate the hanging wall. Black line is the axis of the Tungshih anticline. Black polygons outline the Quaternary fluvial terraces. The river bed was coseismically uplifted along surface rupture scarps by as much as ~10 m during the earthquake (Lee et al., 2005). Black dashed line marks the extent of exposed bedrock reaches along the channel and black square indicates the location of the Da-An River Gorge. Precipitation and discharge records are measured by the Cholan station under the Lanshih Bridge. WFTB – Western Foothills thrust belt; CP – coastal plain.

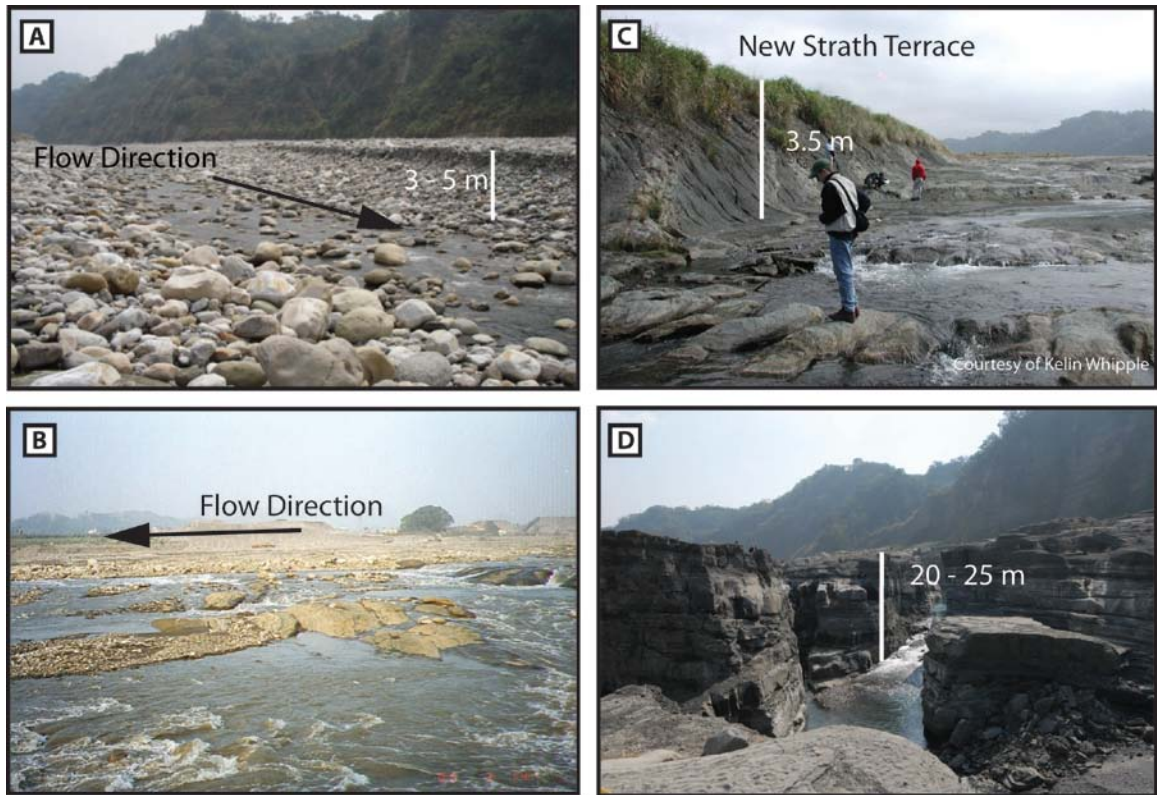


Figure 2. Photographs of the Da-An River in (A) 1998, (B) 2000, (C) 2003 (photograph courtesy of K. Whipple), and (D) 2008. Note that river bed was mantled by 3 to 5 m of alluvium in 1998 and that the alluvial cover was removed and bedrock exposed within six months following the 1999 earthquake. Continued bedrock incision generated a 3.5-m-high strath terrace by 2003 and a 20 to 25 m deep gorge by 2008.

## **CHAPTER 2**

### **STUDY AREA**

#### **2.1 Da-An River**

The 100-km-long Da-An River is a major west-draining fluvial system in western Taiwan with the upper 3/5 of the catchment flowing SW and the lower 2/5 of the basin flowing NNW. The catchment originates in the Hsueshan Range is responsible for draining 760 km<sup>2</sup> of terrain underlain by Oligocene low-grade metamorphic rock and Miocene-Holocene sedimentary rock. A flight of late Pleistocene fluvial terraces are located at the lower reach of the Da-An River, mostly in the north bank (Fig. 1).

The lower half of the Da-An River basin is located in the Western Foothills thrust belt (Fig. 1), where a series of thrust faults have propagated westward since the Pliocene (Ho, 1982). The northern termination of the Chelungpu fault, which crosses the lower Da-An River valley, appears as an anticline in seismic profiles with an exposed bedrock outcrop on the south bank of the Da-An River (Hu and Chiu, 1984). The structural reconstruction of the fold, namely the Tungshih anticline, shows a 400-m-long western limb dipping downstream, a 250-m-long flat top, and a 150-m-long eastern limb dipping upstream on the segment crossed by the Da-An River (Chen et al., 2007). The activation of the Tungshih anticline during the 1999 Chi-Chi earthquake displaced a 1-km-long reach of the Da-An River. This portion of the river valley is characterized by an up-to-3-km-wide floodplain. The alluvium reach has an average slope of 0.014 based on the contours of a 1993 topographic map at a scale of 1:5000.

The denudation rate of the lower Da-An River calculated from suspended sediment yields from 1970 to 1999 is relatively low (~2 mm/yr) in the Taiwan orogen (Dadson et al., 2003). The total suspended sediment discharge in a year for the Da-An River is ~7 metric tons, with 61% of the load associated with typhoon-related flooding

and representing the third highest percentage among all the major rivers in Taiwan (Dadson et al., 2005).

## **2.2 1999 Chi-Chi Earthquake**

The Mw 7.6 Chi-Chi earthquake occurred on September 21, 1999 and is the largest seismic event in Taiwan over the past 100 years (Institute of Earth Sciences, 1999; Ma et al., 1999; Kao and Chen, 2000). The epicenter of the earthquake is located at 23°50'22"N and 121°49'50"E with a focal depth of 8 km (Shin, 2000). The focal mechanism showed a 20° strike and 30° dip with an average rake of 85° (Chang et al., 2000). The earthquake generated over-100-m-long, north-south trending surface rupture in the mountain front (Central Geological Survey, 1999), mainly along the previously mapped Chelungpu fault (Meng, 1963) that produced large earthquakes with an average recurrence interval of ~500 years since 1900 B.P. (Chen et al., 2004). The rupture turned east and northeast into the Western Foothills thrust belt at the south bank of the Da-Chia River valley and ended at the north bank of the Da-An River (Fig. 1). The northern termination of the rupture recorded the maximum values of surface uplift, which are as high as 15 to 16 m in the Da-Chia River valley (Lee et al., 2005). A 5-m high fault scarp knickpoint formed immediately after the earthquake retreated 6 to 20 m within two years (Sklar et al., 2005).

The valley of the lower Da-An River, 29 km from the mouth, experienced uplift along the northern termination of the Chelungpu fault during the 1999 Chi-Chi earthquake. Ground rupture in the vicinity of the Da-An River appeared as a 1-km-wide deformation zone (Fig. 1). The NE-SW (strike is ~55°) trending segment of the Chelungpu fault, which is oriented approximately orthogonal to the Da-An River flow direction is composed of a pair of parallel and outwardly-verging thrust and backthrusts with 50° to 60° dips (Lee et al., 2002). During the Chi-Chi earthquake, the block between the main thrust and the backthrust, was uplifted up to 10 m as the result of the growth of



the Tungshih anticline (Lee et al., 2005). The coseismic uplift in the 1999 earthquake generated a gentler ( $8^\circ$ ) fold scarp on the western limb associated with main thrust and a steeper ( $20^\circ$ ) fold scarp on the eastern limb associated with the backthrust (Chen et al., 2007).

## **CHAPTER 3**

### **METHODS**

The study was conducted along a 7-km-long reach of the lower Da-An River (Fig. 1), where 3 to 5 m of alluvium (Fig. 2A) has been removed and alternating Plio-Pleistocene sandstone, siltstone, and mudstone have been exposed since the earthquake. All the research tasks fall into two categories: (1) the identification of the amount of landscape change, including longitudinal profile evolution and knickpoint migration, and (2) data collection on the hydrometric and the lithological influence of the channel. The investigation will entail a digital elevation model (DEM) analysis consisting of aerial photos, a real-time kinematic global positioning system (RTK GPS) coupled with laser rangefinder surveys, and hydroclimatologic (discharge and precipitation) and lithological data interpretation.

#### **3.1 Digital Elevation Model (DEM) Analysis**

River longitudinal profiles from 1999, 2001, 2002, 2003, 2005, and 2007 were extracted from high-resolution (2 m horizontal) DEMs (Fig. 3). The DEMs were derived by aerial triangulation using stereo pairs of aerial photographs taken by the Agricultural and Forestry Aerial Survey Institute of Taiwan. Two software programs were used in image processing to produce DEMs with the highest possible resolution. We used ERDAS IMAGINE software to build the interior and exterior orientations by entering camera calibration information provided by the Agricultural and Forestry Aerial Survey Institute and ground control points acquired from a RTK GPS system with horizontal and vertical uncertainties of 14 mm and 24 mm, respectively. After performing aerial triangulation, the exterior orientation and updated latitude, longitude, and elevation of each aerial photograph were the inputs for the Inpho ApplicationsMaster software

package, which in our case allowed generation of DEMs with grid sizes in the range of 1.19 to 2.74 m. For the simplification of the DEM-based analyses, we resampled the grid size of each DEM to 2 m x 2 m pixels.

The aerial photographs from which the DEMs were made were also used to extract longitudinal profiles precisely and calculate knickpoint migration rates. We orthorectified and georeferenced these aerial photographs, which have horizontal resolutions of 0.26 to 0.48 m, by ERDAS IMAGINE software. The orthorectified aerial photographs were overlaid on the DEMs in ArcGIS to aid in the extraction of grid points in the river valley. The aerial photographs allowed us to ensure that every point extracted was located in the channel. In addition, an orthorectified aerial photograph was used as a base image (Fig. 4A) on which we mapped the historical knickpoints from a series of DEMs to track the trace of propagation and calculated its rates (Fig. 4B).

### **3.2 Global Positioning System Channel Surveys**

Four river longitudinal profiles were surveyed from 2008 to 2009 by a RTK GPS coupled with a laser rangefinder, which was used for inaccessible places, to quantify the morphological change of in the Da-An River channel between the wet and dry seasons. We focused on a 7-km-long reach of the lower Da-An River (Fig. 1), where the channel is actively incising and where bedrock is exposed. The water levels of the river were surveyed instead of the channel bottoms, which were inaccessible in many reaches. We entered the river valley during the low flow regime to minimize the effect of water level fluctuation, which is approximately  $\pm 0.25$  m during the dry season according to our repeat survey of same points in different days. Therefore, when plotting the time-series of the longitudinal profiles from 1999 to 2009, any vertical change in the water levels are negligible compared to the amount of bedrock incision that occurred (Fig. 5A).

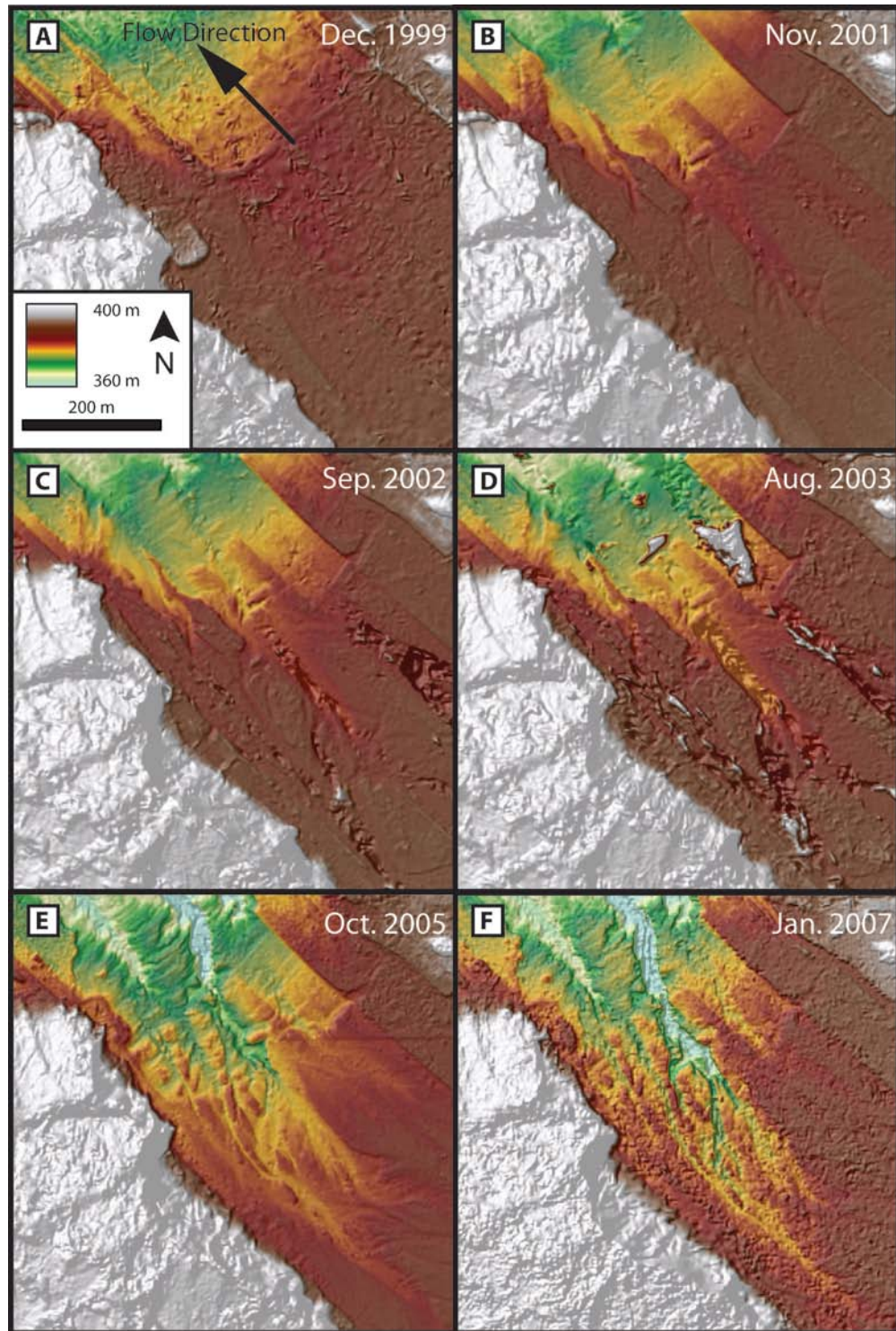


Figure 3. Time series of aerial photograph-derived digital elevation models used for longitudinal profile extraction and knickpoint migration measurements (A-F). The aerial photographs are provided by the Agricultural and Forestry Aerial Survey Institute of Taiwan. Note that the bulges on the NW bank of the river in the 2003 image are sediments piled up by a gravel mining operation. Please see Figure 1 for the location.



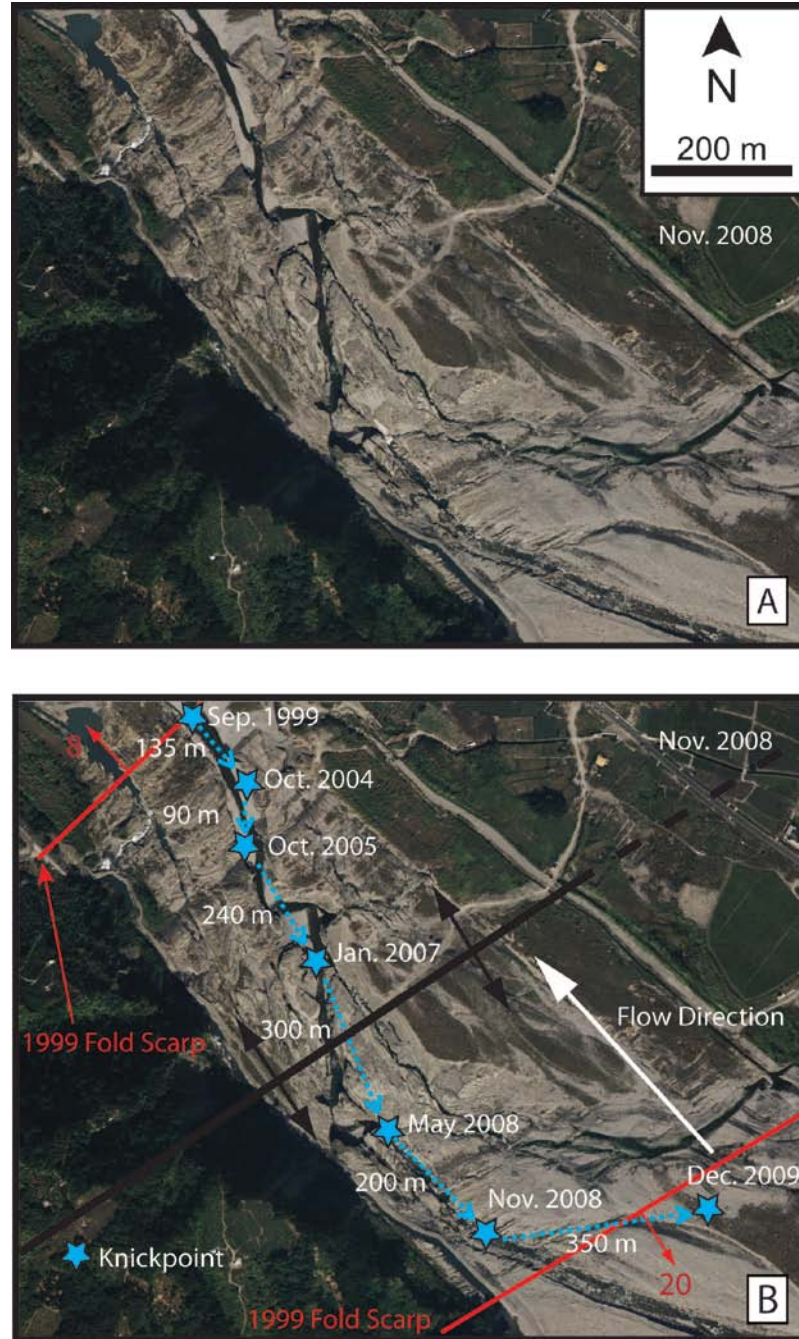


Figure 4. (A) An example of orthorectified aerial photographs provided by the Agricultural and Forestry Aerial Survey Institute of Taiwan for analyzing spatial-temporal changes of the lower Da-An River segment (please see Figure 1 for location). (B) Trace of the 1999 fold scarps and location of the Da-An River knickpoint by year using A as a base map. Black line is the axis of the Tungshih anticline. Red lines are a set of fold scarps which accommodated 1999 Chi-Chi surface deformation. The dips and dip orientations are indicated by red arrows and numbers adjacent to them (Chen et al., 2007). Blue stars mark the locations of historical knickpoints determined by a time series of river longitudinal profiles extracted from aerial photograph-derived DEMs (Fig. 3) and surveyed by a real-time kinematic global positioning system (RTK GPS). Blue dashed lines present the traces, directions and distance of knickpoint migration.

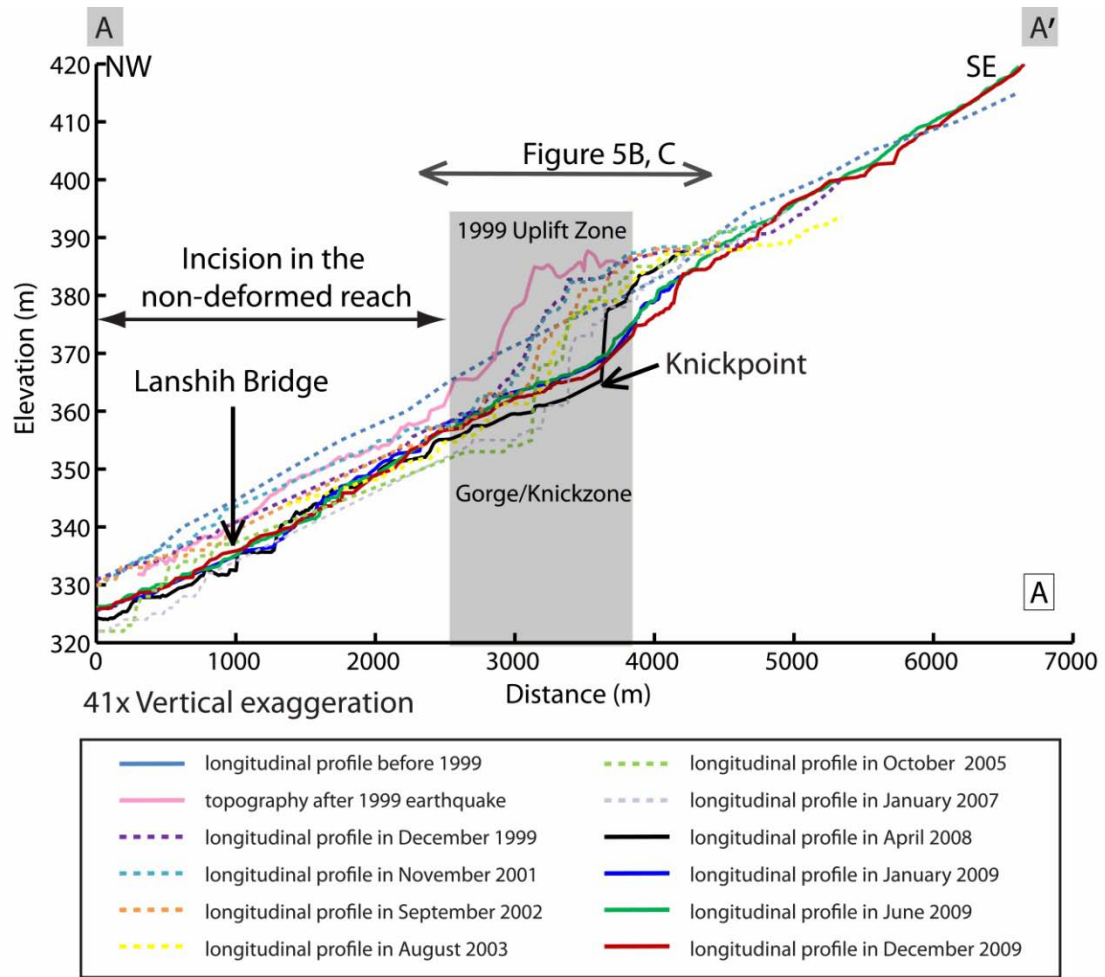


Figure 5 continued

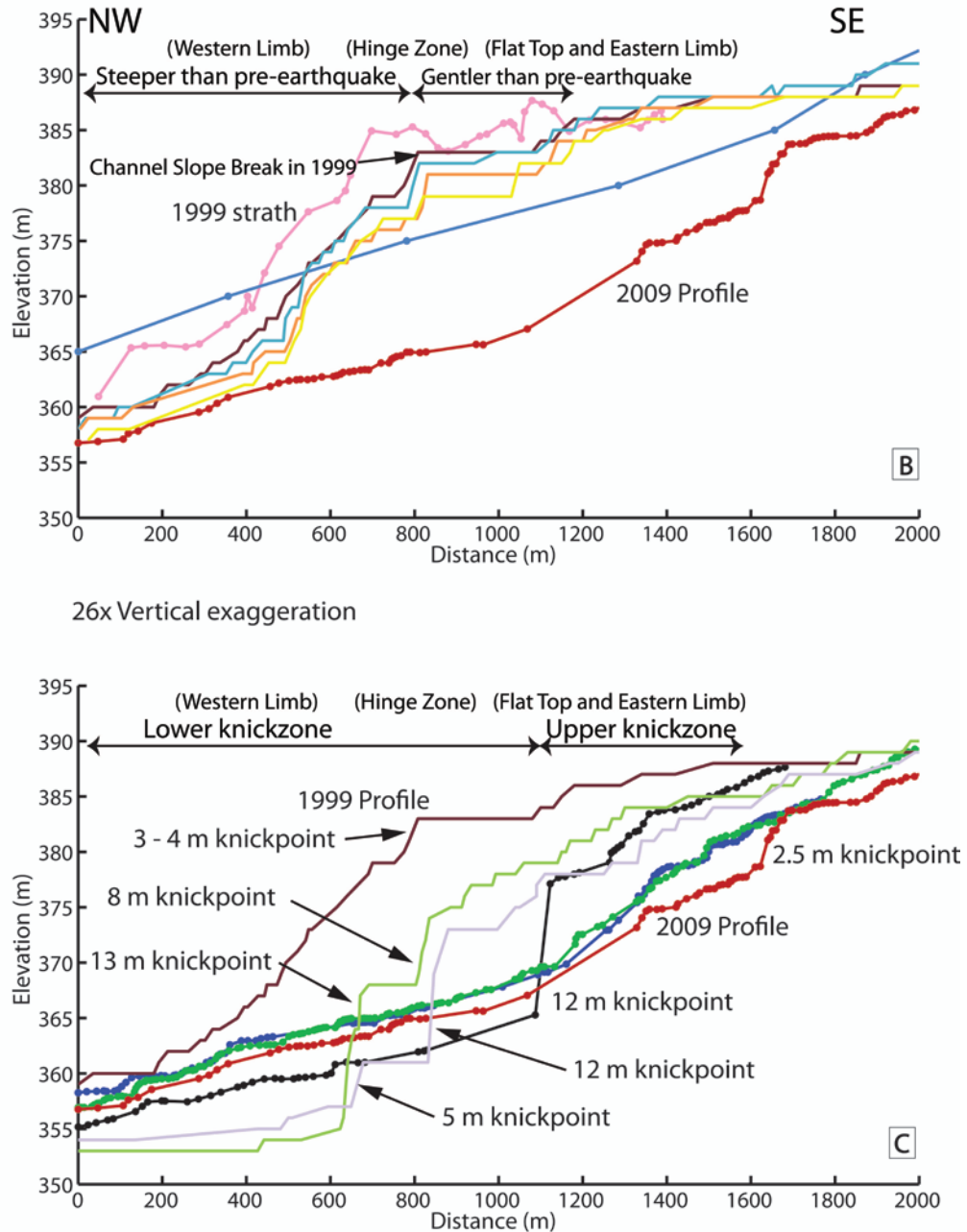


Figure 5. (A) Evolution of the longitudinal profile of the Da-An River from 1993 to 2009. (B) and (C) Close-up view of the longitudinal profiles evolution in the 1999 Chi-Chi earthquake uplift zone for the period of 1993 to 2003 (B) and 2005 to 2009 (A). The pre-earthquake profile (1993) is based on the contours of a 1993 1:5,000 scale topographic map produced from aerial photographs. The post-earthquake topography is inferred from a strath terrace profile surveyed using a RTK GPS in May, 2008. The river longitudinal profiles before 2008 are extracted from aerial photograph-derived DEMs. The profiles of April, 2008; January, 2009; June, 2009; and December, 2009 are based on RTK GPS surveys. Please see Figure 1 for the location.

### **3.3 Precipitation and Discharge**

Daily measurements of precipitation and discharge of the study reach are recorded at the Cholan station under the Lanshih Bridge (Fig. 1), which was set up by the Water Resource Agency. The records from this gauging station extend back to 1903 for rainfall and 1973 for discharge. However, the discharge data after 2005 is not available because of numerous errors in data collection (Fig. 6). In addition, the Cholan station was removed after June, 2006 as the result of Langshih Bridge reconstruction. Another meteorology station on the south end of the Lanshih Bridge, owned by Central Weather Bureau, provides daily and hourly precipitation data, which are very useful for analyzing rainfall intensities of each typhoon.

We summed the daily precipitation and averaged the daily discharge records to obtain monthly precipitation and discharge over the period 1999 to 2009 (Fig. 6). In order to clarify the climatic influence on channel change in terms of flooding events, we used precipitation as a proxy of discharge to sort out the major flooding events because the discharge data after January 1, 2005 are not available. Each flooding event is defined by one or more consecutive days of precipitation. We choose events with daily precipitation > 111 mm as major flooding events and 18 major flooding events were determined from 1999 to 2009. The total precipitation, the maximum daily precipitation, and the maximum hourly precipitation of each event are listed in Table 1.

### **3.4 Rock Strength and Joint Orientations**

Rock strength and strike and dip of joint planes and bedding planes were measured to clarify the lithologic influence on the rates and the patterns of bedrock incision (Fig. 7; Table 2). The exposed bedrock in the study area is weakly-cemented siliclastic Plio-Pleistocene sedimentary rocks of the Western Foothills thrust belt (Fig. 1). To calibrate the effect of lithology on bedrock incision, a concrete test hammer (Schmidt Hammer) was used to measure the compressive strength of bedrock. More than 100



rebound values in total were recorded on mudstone, siltstone, and sandstone along the flow path. We used the rebound value-compressive strength graph provided by the manufacturer to correct for the impact positions and to determine the compressive strength of the various lithologies.

More than 1,200 joint plane orientations (strike and dip) were measured using a Brunton compass. The uncertainties of measurements taken by this compass are approximately  $\pm 2.5^\circ$ . These data are from 22 sites in the Da-An River gorge (Fig. 4A); 12 sites are located on north bank and eight on south bank of the Da-An River. Approximately 50 strike and dip measurements were collected at each site.

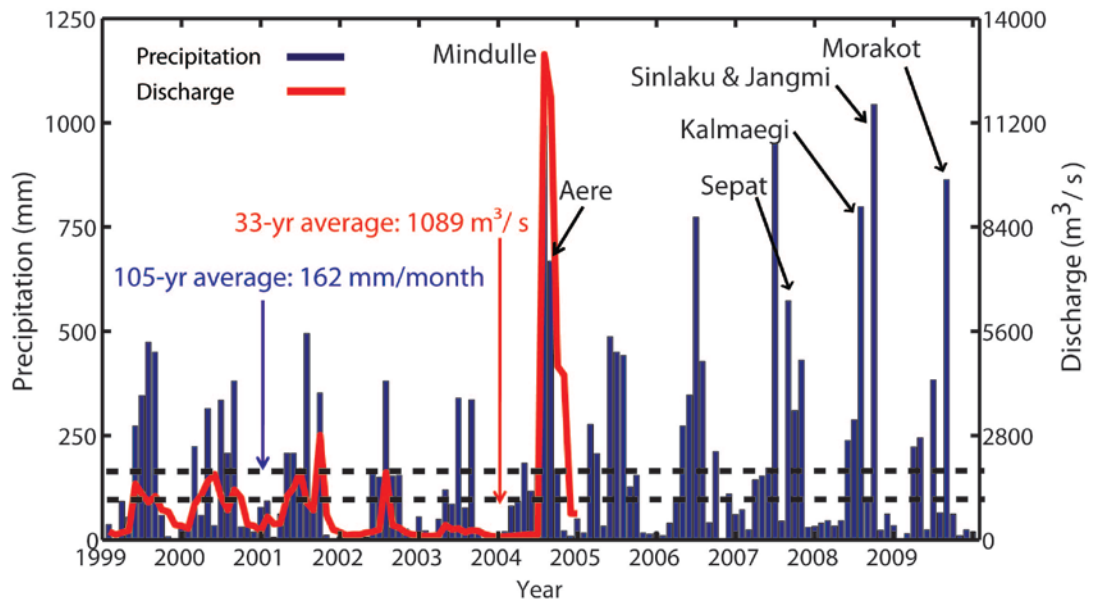


Figure 6. Monthly average precipitation and discharge for the period 1999 to 2009 along the lower Da-An River as measured at the Cholan station settled by Water Resource Agency of Taiwan (Fig. 1). Dashed lines represent the average monthly precipitation and average discharge for the examined period. Six of eight months with precipitation  $> 500$  mm are associated with typhoons with their names as shown. The months with the highest precipitation and discharge during this time span are approximately six and ten times the average. Post- 2005 discharge data are not shown because the data after January, 2005 are erroneous with  $> 1000$   $\text{m}^3/\text{s}$  daily discharge in the dry seasons (November - April). The data after June, 28 2006 are unavailable due to the removal of the Cholan station.

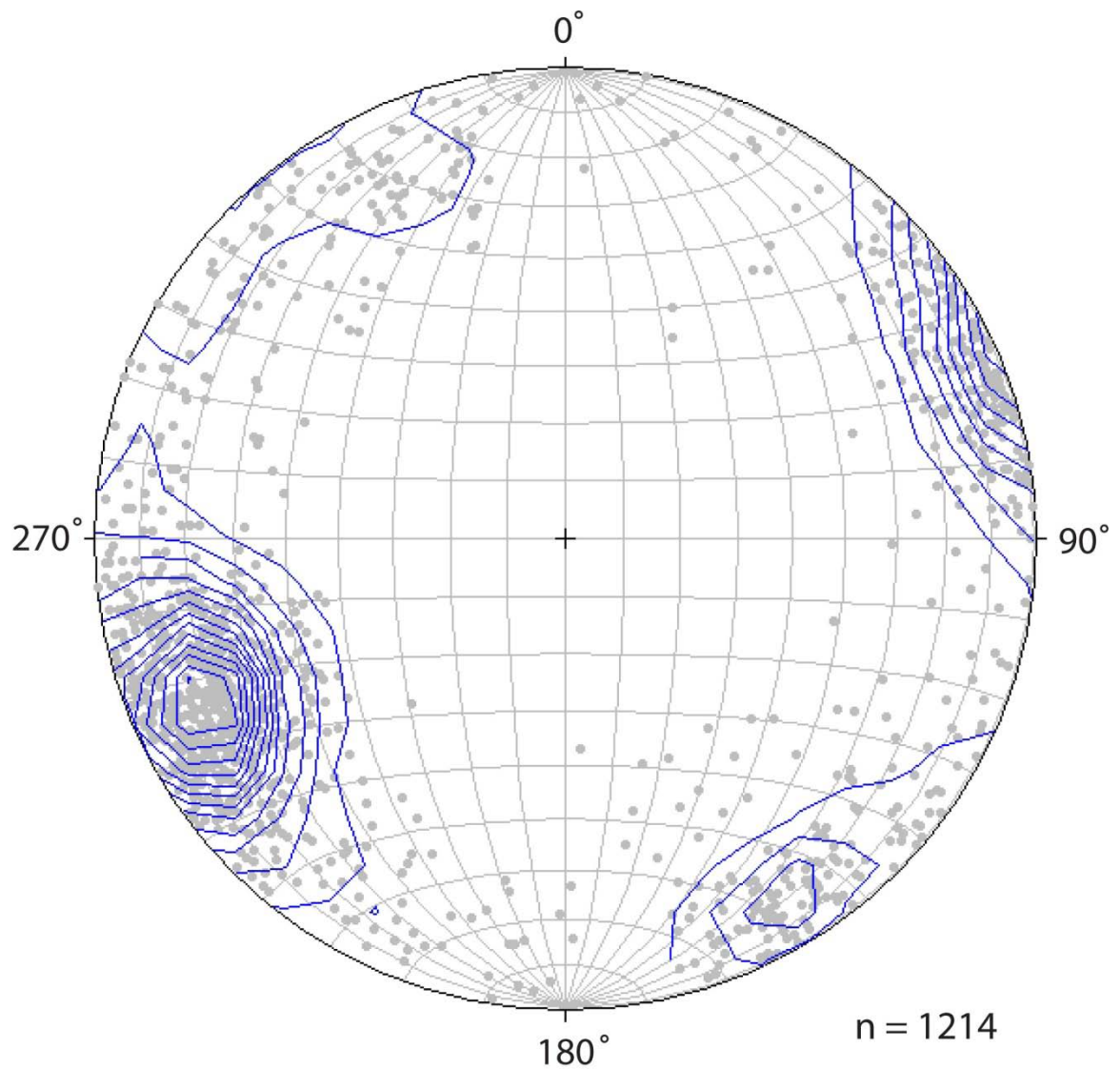


Figure 7. Equal area stereonet contour plot of poles to 1214 measured joint planes in the Da-An River Gorge using Stereonet program provided by Rick Allmendinger's website ([www.geo.cornell.edu/geology/faculty/RWA/programs.html](http://www.geo.cornell.edu/geology/faculty/RWA/programs.html)). Note that the dominant NE-SW joint orientation closely matches the channel pattern in the Da-An River (e.g., Fig. 4A).

Table 1. Hydroclimatological data of major flooding events in western Taiwan, 1999 - 2009

Year	Date (mm/dd)	Name of Typhoon /Event <sup>+</sup>	Total Precipitation (mm)	Maximum Daily Precipitation (mm)	Maximum Hourly Precipitation (mm)	Maximum Daily Discharge* (m <sup>3</sup> /s)	Impact
2001	07/29-07/30	Toraji	367	365	86.5	168	
2001	09/16-09/18	Nari	276	120	38.5	1190	
2004	07/01-07/06	Mindule	765	263	104.5	2686.5	
2004	08/23-08/29	Aere	521	271	65.0	N/A	Major knickpoint appeared
2005	05/12-05/15	heavy rain	351	185	49.0	N/A	
2005	06/10-06/17	heavy rain	242	113	24.5	N/A	
2005	07/17-07/22	Haitang	441	219	42.0	N/A	Bedrock under the Lanshih bridge exposed
2005	08/03-08/06	Matsa	339	198	35.5	N/A	
2006	04/10-04/11	heavy rain	115	114	38.0	N/A	
2006	05/27-06/13	heavy rain	887	174	61.5	N/A	Lanshih bridge broken
2006	07/13-07/15	Bilis	234	191	34.5	N/A	alternative bridge broken
2007	06/03-06/10	heavy rain	684	228	46.0	N/A	
2007	09/17-09/19	Wipha	201	187	25.0	N/A	Lanshih bridge closed; alternative bridge submerged and broken
2007	10/06-10/08	Krosa	430	254	41.5	N/A	Lanshih bridge closed
2008	07/17-07/20	Kalmaegi	386	330	80.5	N/A	
2008	09/12-09/16	Sinlaku	664	435	52.0	N/A	
2008	09/28-09/30	Jangmi	273	218	33.5	N/A	
2009	08/05-08/10	Morakot	745	402	55.0	N/A	

Note: <sup>+</sup>With maximum daily precipitation recorded in Cholan Meteorological Station >111 mm.

\*Daily discharge data after January, 2005 are erroneous with > 1000 m<sup>3</sup>/s daily discharge in the dry seasons (November - April), after June, 28 2006 are unavailable

Table 2. Amount of knickpoint migration during the wet seasons (May-October, 2005-2009) and average dip of the bedrock bedding planes in which knickpoint migrated

Year	Knickpoint Migration (m)	Bedding Dip (°)
2005	90 ± 10	22.0 ± 2.5
2006	240 ± 10	16.0 ± 2.5
2007	310 ± 10	6.5 ± 2.5
2008	200 ± 10	24.0 ± 2.5
2009	350 ± 10	3.0 ± 2.5

## CHAPTER 4

### RESULTS

#### 4.1 Evolution of Longitudinal Profiles

Combining data from topographic maps, DEMs and RTK GPS surveys yield a time series of longitudinal profile change of the Da-An River prior to, and following, the 1999 Chi-Chi earthquake (Fig. 5A). A 1-km-long reach of the Da-An River with a pre-displacement slope of 0.014 experienced surface uplift of ~10 m (Lee et al., 2005) above a fault propagation fold (the Tungshih anticline) during the Chi-Chi earthquake. Following the earthquake, the longitudinal profile was characterized by a convex-upward shape with a sharp break in slope in the anticlinal hinge zone between the western limb and the flat top (Fig. 5B). This break in slope separated an 800-m-long reach that was steeper than its pre-earthquake gradient in the western fold limb with a 450-m-long reach that was gentler than its pre-earthquake morphology on the flat top and eastern fold limb. In a prominent contact between resistant siltstone and nonresistant mudstone in downstream-dipped strata, a 3- to 4-m-high knickpoint formed below the slope break immediately following the earthquake (Fig. 5C).

The rates of fluvial incision in the Da-An River were not steady in the postseismic years. In the period of 1999-2004, the bottom of channel was lowered 6 to 9 m (Fig. 5B) with 3 to 5 m of alluvium removed (Fig. 2B) and the formation of a series of 3- to 4-m-high strath terraces above the channel bed (Fig. 2C). Accordingly, the incision rate in this time frame is about 1.2 to 1.8 m/yr. In addition, the height and position of the knickpoint did not change significantly (< 100 m migration in 5 years) during this time span (Fig. 5B).

The beds of the trunk channel of the Da-An River were incised dramatically in the period from 2005 to 2009. Therefore, a more than 20-m-deep bedrock gorge was formed. In 2005, two major knickpoints were developed in the trunk channel: 1) the pre-existing one in the lower part of the uplifted reach, which increased in height to 8 m (Fig. 5C), and 2) a new 13-m-high knickpoint, which developed in below the pre-existing knickpoint. Above the 8-m-high knickpoint, the gradient of the 500-m-long reach had increased from 0.006 as measured in 2003 to 0.016. Below the 13-m-high knickpoint, up to 7 m vertical incision and the extension of the bedrock exposure to the reach 3-km downstream from the coseismic uplift, was found (Fig. 5A). The longitudinal profile in January 2007 shows that both knickpoints propagated upstream in 2006 with a 5-m-high knickpoint developed below a 12-m high knickpoint. The propagation was accompanied by ~2 m aggradation and ~5 m incision along the 600-m long reach below and above the knickpoint zone, respectively. The knickpoint continued to propagate in 2007, which generated fluvial hanging valleys from tributary channels along the gorge wall (Fig. 8B). A knickpoint with the height of 12 m is apparent in the longitudinal profile surveyed after the 2007 propagation (Figs. 5C and 8C).

The height of knickpoint decreased to < 5 m in the longitudinal profiles surveyed during 2009 (Fig. 8C). The longitudinal profile surveyed in January, 2009 indicates the collapse of the previous 12-m-high knickpoint, 3 to 4 m of aggradation below the toe of the knickpoint (Figs. 9A and 9B), and 7 to 8 m of incision upstream of the waterfall (Figs. 9C and 9D) in the second half of 2008 (Fig. 5C). The extent of the aggradation and the incision were 1,500 m downstream and at least 600 m upstream from the decayed knickpoint, respectively. Therefore, the collapse of the 12-m-high knickpoint dramatically smoothed the longitudinal profile, which began transformation to a concave-up channel with knickpoints less than 3 m in height by January, 2009 (Fig. 5C). In addition, the limit of the bedrock exposure extended 370 m upstream as the result of the 7 to 8 m incision in the reach upstream from the collapsed knickpoint. In 2009, the

elevation of the channel bed did not change significantly until the second half of the year. The longitudinal profile surveyed in December, 2009 shows up to 5 m, downstream-decreased vertical incision in the whole 1.4-km long knickzone (Fig. 5C). The along-knickzone incision in summer, 2009 caused the limit of the bedrock exposure to extend 300 m further upstream and formed a 2.5-m-high knickpoint(Figs. 5C and 8D), which is located outside of the 1999 uplifted zone (Fig. 4B). The lower knickzone (Fig. 10D), which underwent incision from 1999 to 2004 (Fig. 5B) and aggradation from 2005 to 2009 (Figs. 5C, 9A, and 9B), began incising again.

In the end of 2009, the incision and bedrock exposure had extended 700 m and 2,500 m upstream and downstream from the 1999 deformation zone, respectively. The area between the unaltered alluvial reaches upstream and downstream of the gorge can be classified into four segments (Fig. 10A): 1) a bedrock-exposed reach 700 m upstream from the gorge with an average gradient of 0.02 (Fig. 10B), 2) a 300-m-long upper knickzone dominated by cascade and step-pool reaches, where the channels are incising and narrowing actively with an average gradient of 0.024 (Fig. 10C), 3) a 1100-m-long lower knickzone, where incised channels are filled with 3 to 4 m alluvium as result of aggradation with an average gradient of 0.011 (Fig. 10D), and 4) a sediment-filled bedrock reach 2,500 m downstream from the gorge with an average gradient of 0.012 (Fig. 10E).

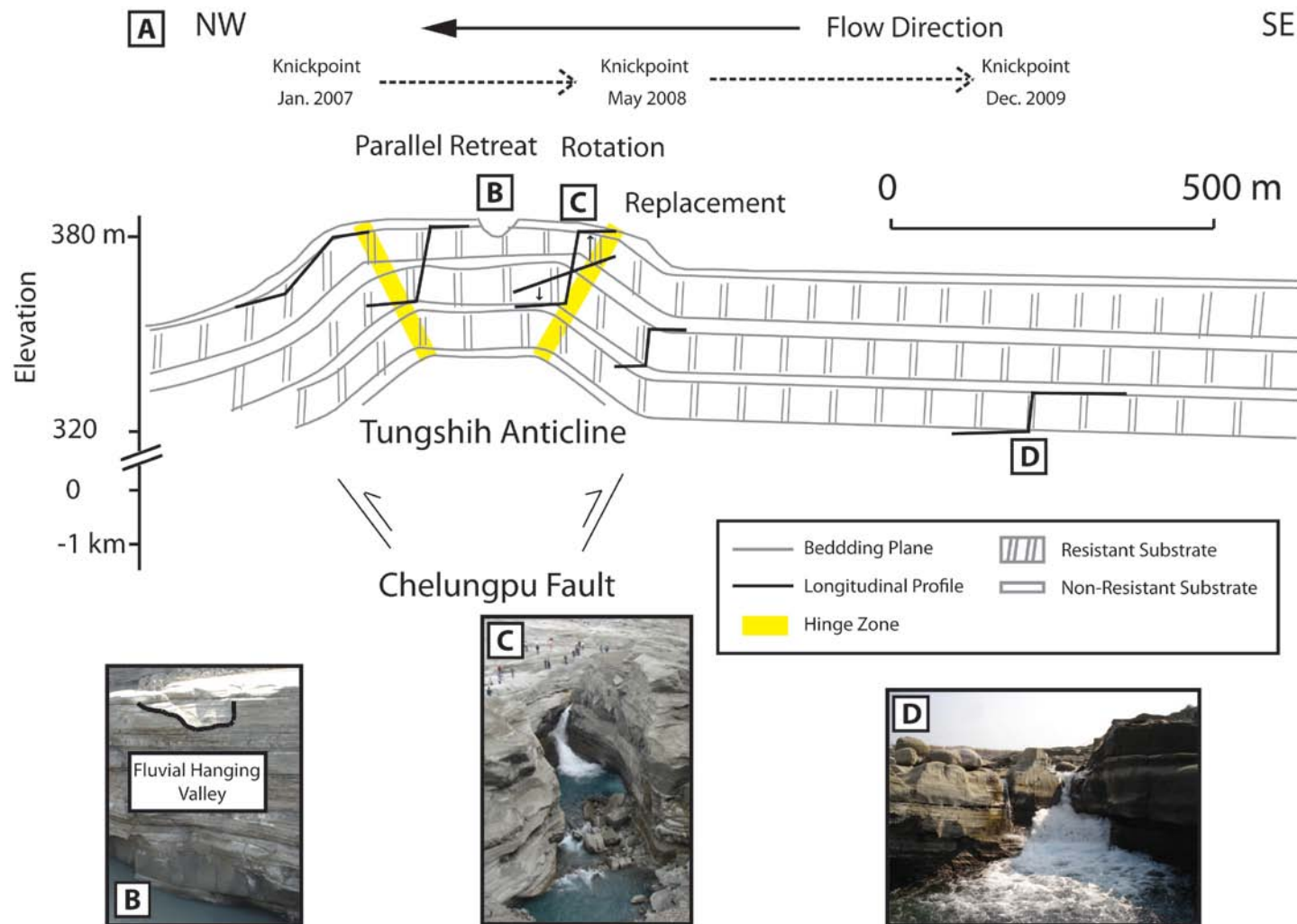


Figure 8. (A) Schematic diagram illustrating how the Da-An River knickpoint migrates through the Tungshih anticline. Subsurface structure modified from Chen et al. (2007). Field photographs showing fluvial hanging valley (B) left in the gorge wall and knickpoints in (C) March, 2008 and (D) December, 2009. Letters on cross-section in A correspond to field photographs B, C, and D.



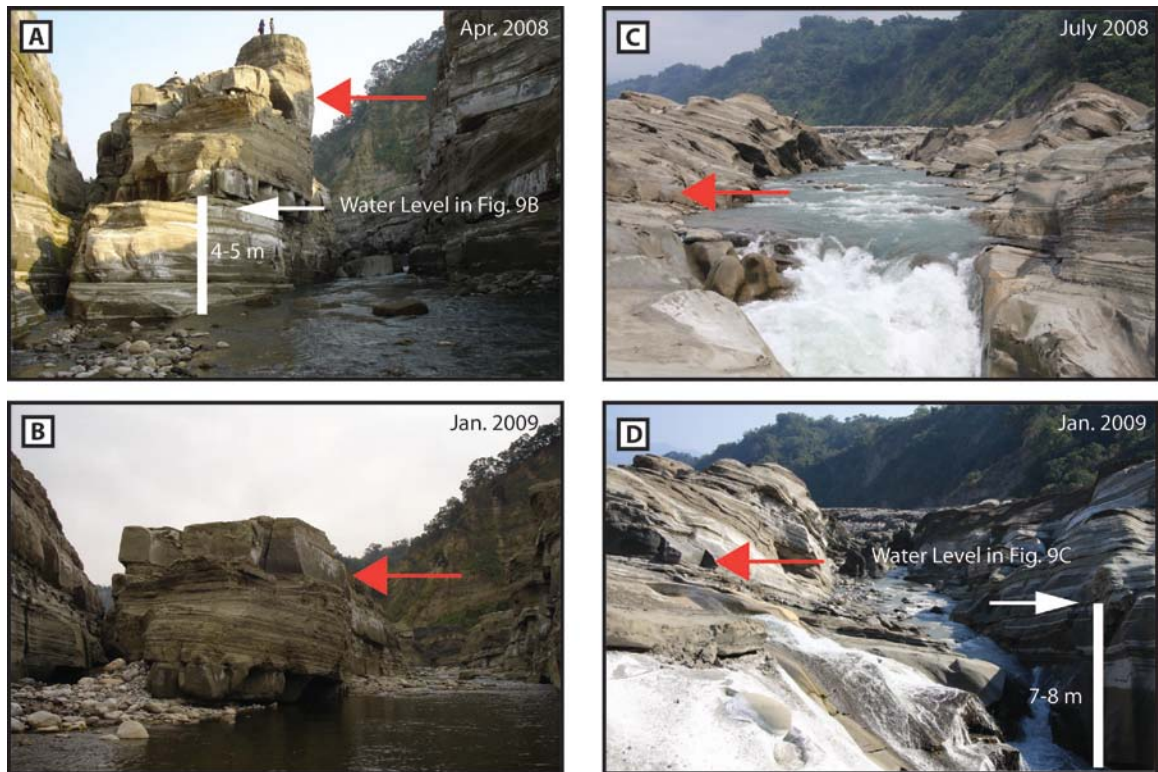


Figure 9. Photographs looking upstream of dramatic aggradation between April, 2008 and January, 2009 (A and B). Photographs C and D illustrate incision in the knickzone following three typhoon-triggered floods in summer, 2008 (Fig. 6 and Table 1). Red arrows point to the same strata in both pairs of the photographs.

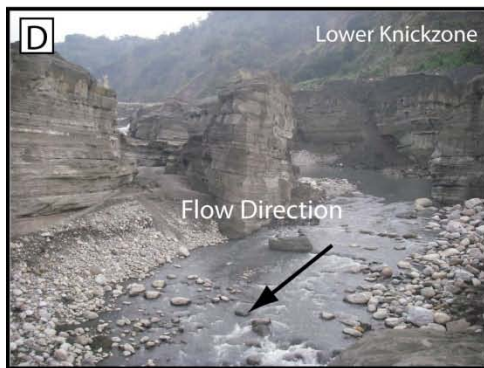
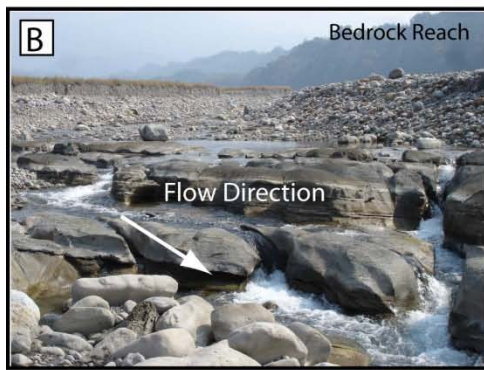
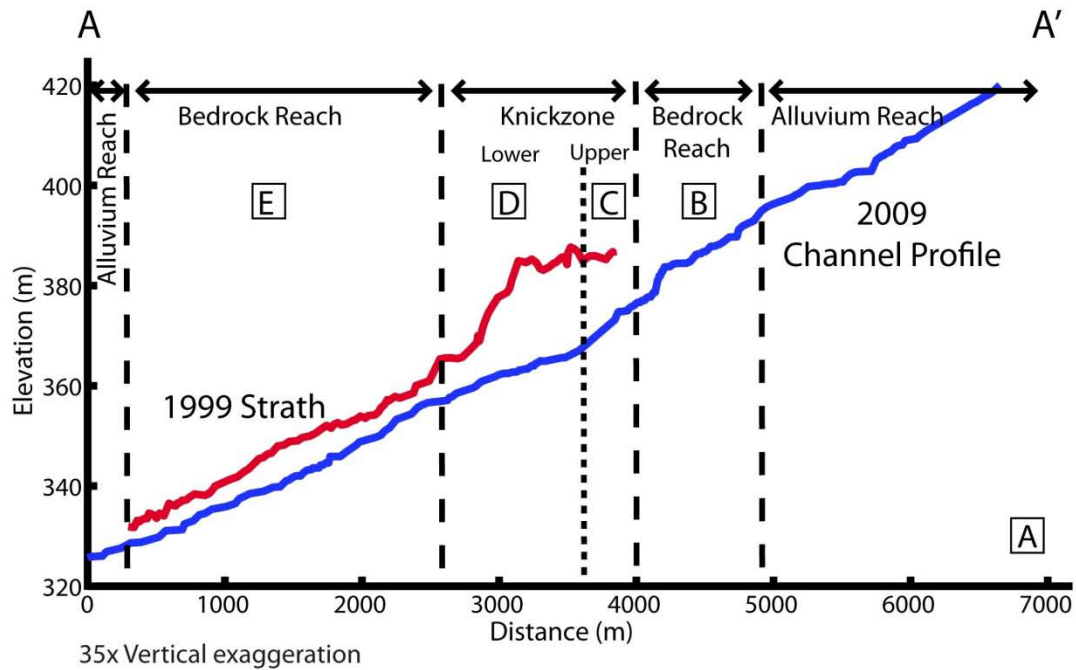


Figure 10. (A) A longitudinal profile, strath terrace profile, and photographs of the Da-An River show the location and morphology of four classified reaches in the study area. (B) A bedrock-exposed reach 700 m upstream from the knickzone. (C) A 300-m-long upper knickzone dominated by cascade and step-pool reaches, where the channels are incising and narrowing actively. (D) A 1100-m-long lower knickzone, where incised channels are filled with 3 to 4 m alluvium as result of aggradation. (E) A sediment-filled bedrock reach 2,500 m downstream from the knickzone. Letters on longitudinal profile in A correspond to field photographs B, C, D and E.

## **4.2 Precipitation and Discharge**

The long-term average annual rainfall and the daily water discharge recorded at the Cholan station (Fig. 1) are 1948 mm/yr and 36 m<sup>3</sup>/day, respectively (Hydrological Yearbook of Taiwan, R.O.C, 1904-2008). The records of both rainfall and discharge reflect seasonal changes (Fig. 6). Precipitation records show that 78% of the annual precipitation occurs between May and October. Discharge during typhoons can exceed the daily average by almost two orders of magnitude (Fig. 6). For example, in August 2000, Typhoon Mindulle produced a flood in the Da-An River peaking at 2,687 m<sup>3</sup>/s (Table 1), or about 74 times the daily average discharge, which ranks second over the 32 years of records.

After 1999, the first four years are “dry” years, where the annual precipitation is below the 105-year average (Fig. 6). Since then, however, the annual precipitation has been 1.2 to 1.5 times greater than the long-term average (Fig. 6). More frequent floods were reported over the period 2004 to 2009 with 16 of 18 major flooding events in which daily precipitation had exceeded 111 mm, the maximum daily precipitation recorded with no significant changes in the trunk channel of the Da-An River, from 1999 (Table 1). Most of the major events, occurred between July and October, are associated with typhoons (Fig. 6).

## **4.3 Bedrock Structure**

### **4.3.1 Rock Strength**

We measured compressive strength on sandstone (n = 7), siltstone (n = 91), and mudstone (n = 17) beds exposed near the Da-An River gorge. Siltstone and mudstone were the most common bedrock that appeared on the reach; however, the latter was too weak to generate rebound values > 10 N/mm<sup>2</sup>, which is the minimum reliable rebound value. Thus, only a few measurements were taken. The compressive strength for

sandstone, siltstone, and mudstone in the study area are similar and range from 8.6 to 25.4 MPa, 2.6 to 54.8 MPa, and 5.3 to 18.1 MPa, respectively. No spatial variation in rock compressive strength was found along the study reach.

#### **4.3.2 Joint Orientations**

We collected 1214 joint orientation measurements across all rock types (sandstone, siltstone, and shale) along the incised reach of the Da-An River, where the gorge is formed (Fig. 4A). Joint planes strike predominantly  $340^{\circ}$  and  $55^{\circ}$  with dips ranging from  $37^{\circ}$  to  $90^{\circ}$  (Fig. 7). More than 75% of measurements in both sets of joint planes are high angle with dips in the range of  $70^{\circ}$  to  $90^{\circ}$  (Fig. 7). The strike of the most dominant set of joint planes ( $340^{\circ}$ ) is close to the local flow direction of the incised Da-An River channel.

#### **4.3.3 Bedding Dip**

The knickpoint stayed at the original downstream end of the fold scarp until 2004 (Fig. 4B), after which it propagated  $\sim 1,190$  m upstream (Table 2; Fig. 4B), yielding a mean migration rate of 238 m/yr from 2005 to 2009. By the end of 2009, the knickpoint was located in horizontally-layered bedrock (Figs. 8A and 8D) upstream from the anticline and 1999 deformation zone (Fig. 4B). The migration crossed the Tungshih anticline in which the dip of bedding ranges from  $0^{\circ}$  to  $45^{\circ}$  (Chen et al., 2007). Based on field measurements and observations, knickpoints appear to migrate faster through flat-lying strata than tilted strata (Fig. 11).

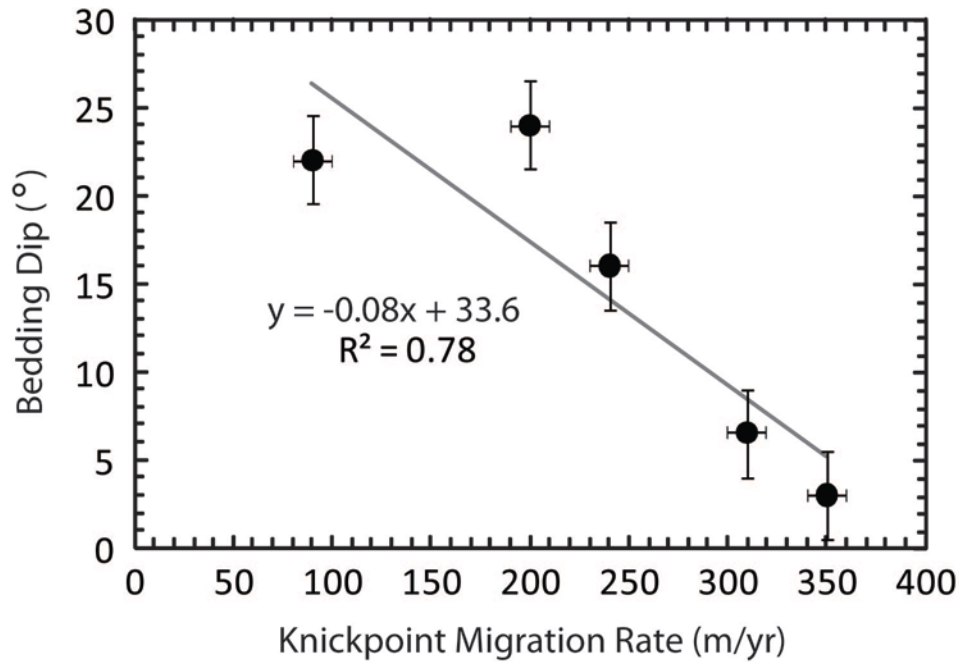


Figure 11. Linear regressions performed on knickpoint migration rate as a function of bedding dip within the Tungshih anticline. The uncertainties for dip and knickpoint migration rate are  $\pm 2.5^\circ$  and  $\pm 10$  m/yr, respectively.

#### 4.4 Knickpoint Migration Rates

The trace and the amount of knickpoint migration are presented in Figure 4B. Two distinct knickpoint migration rates were found from 1999 to 2009. The knickpoint that formed immediately after the earthquake migrated 135 m in the downstream end of the fold scarp and yielded a migration rate of 27 m/yr for the period from 1999 to 2004. Between 2005 and 2009, the knickpoint migrated 1190 m across the anticline, exhibiting a migration rate of 238 m/yr. This number is almost an order of magnitude of faster than the knickpoint migration rate in the first five years after the earthquake.

Non-uniform knickpoint migration rates were reported when knickpoints propagate across the different portions of the Tungshih anticline (Fig. 4B; Table 2). The migration is relatively slow (90 m/yr) in the western limb of the anticline where bedrock dips  $20^\circ$  to  $25^\circ$  to the west. The rate of retreat increased to 240 m/yr when knickpoints traveled upstream through a hinge zone with gentler bedding dips ( $13^\circ$  to  $18^\circ$ ). Then the

velocity of migration reached peak values (310 m/yr) within the flat top of the anticline where dips are consistently less than  $10^\circ$ . The knickpoint propagation slowed down (200 m/yr) in the eastern limb of the anticline with an average dip of  $24^\circ$  to the east. Afterward, rates of knickpoint migration peaked again (350 m/yr) in the horizontal strata upstream from the anticline.

## CHAPTER 5

### DISCUSSION

#### 5.1 Tectonic- and Climate-Driven Bedrock Incision

Our results show tectonics and climate directly contribute to the observed ultra-high rate of fluvial incision in the Da-An River, which is in a good agreement with the controls on decadal-scale denudation rates in Taiwan (Dadson et al., 2003). The coseismic uplift of the 1999 earthquake locally doubled the channel gradient and lowered base level for the uplifted reaches (Fig. 5A). Following the uplift, climate-triggered floods accelerated the pace of the fluvial response to the new boundary condition (Fig. 6; Table 1).

Base level fall was exacerbated by active incision in the 3-km-long reach immediately downstream from the 1999 deformation zone following the earthquake (Fig. 5A). The additional lowering occurred in the non-deformed reach because the flow velocity, which is a power function of shear stress (Stein and Julien, 1993), remained high after the acceleration on the fold scarp facing downstream (Fig. 5B). The shear stress on the channel bed exceeded the critical value required for initiating incision. The lowering of the non-deformed downstream reach generated base level fall in addition to coseismic uplift. This explains the “excess” bedrock incision in the Da-An River gorge, where the amount of fluvial incision (>20 m) exceeded the coseismic uplift (~10 m). The channel beds were below their pre-earthquake levels after undergoing excess erosion in response to the coseismic uplift (Fig. 5B).

Climate played an important role in controlling the response time. Floods associated with large precipitation events accelerated the pace of the downcutting in the Da-An River valley during the post-earthquake period. Similar trends between the post-

earthquake river incision and precipitation records suggest that climate plays an integral role on the fluvial response to coseismic uplift. The Da-An River experienced two stages of fluvial incision, which are coincident with variations in annual precipitation records. Moderate vertical incision (1.5 to 2.25 m/yr) and knickpoint migration (27 m/yr) occurred from 1999 to 2003 (Fig. 5B), corresponding to the years with annual precipitation below the 105-year-average (Fig. 6). Extremely high rates ( $>10$  m/yr) of bedrock incision, rapid knickpoint migration (238 m/yr) and the formation of the gorge occurred from 2004 to 2009 (Fig. 5C), corresponding to the years with precipitation levels 1.2 to 1.5 times greater than the 105-year average (Fig. 6). More frequent typhoon-associated floods and flooding events in which precipitation exceeded 111 mm in one day also occurred during these years (Table 1). During 2009 there was only one major flooding event with daily precipitation more than 400 mm (Fig. 6; Table 1). However, significant channel incision was found in the knickzone during the same time span (Fig. 5C). Therefore, it appears that the intensity of individual storms, instead of annual precipitation increase, was primarily responsible for the rapid incision. The occurrence of frequent floods during 2004 to 2008 was reflected in above-average annual precipitation.

The aerial photographs show that a series of knickpoint migrations and rapid bedrock incision were initiated during the flood triggered by Typhoon Mindulle in July, 2004, the largest flood since 1982. The peak discharge of the July, 2004 flood event was  $2,687 \text{ m}^3/\text{s}$  following peak rainfall of 105 mm/hour, both of which were the highest values recorded during our observation period (1999 to 2009) (Table 1). Before the substantial knickpoint migration in 2004, only two flooding events were found (Table 1), which initiated no significant incision and knickpoint migration during the dry years (Fig. 5B). This suggests a threshold value between 1200 and  $2600 \text{ m}^3/\text{s}$  for initiating the ultra-high rates of bedrock incision and knickpoint migration in the Da-An River gorge. The lower limit of the threshold discharge is determined from the fact that no day in dry years has maximum daily discharge more than  $1200 \text{ m}^3/\text{s}$  (Table 1), thus no apparent



knickpoint migration would occur when daily discharge  $< 1200 \text{ m}^3/\text{s}$ . The upper limit for the threshold is based on the fact that knickpoint retreat increased significantly ( $90 \text{ m/yr}$ ) in 2004 after a flood with maximum daily discharge  $>2600 \text{ m}^3/\text{s}$  (Table 1). Thus, the knickpoint would propagate remarkably when daily discharge  $> 2600 \text{ m}^3/\text{s}$ .

In addition, we observed that significant changes in longitudinal profiles occurred only in flooding events with a precipitation rate greater than  $111 \text{ mm/day}$ . The results of our RTK GPS survey covering a dry season (January, 2009 to June, 2009) with maximum daily precipitation of  $111 \text{ mm}$  show almost no change in channel elevation (Fig. 5C), suggesting that substantial channel incision and deposition do not occur during the dry season. Furthermore, the channels were not altered every day during the wet season. Field observations indicate that the channels did not change during the wet season of 2009 until the first flooding event in which the Cholan station received  $402 \text{ mm}$  precipitation in a day from Typhoon Morakot (Table 1). Because it is the only large flooding event of 2009 (Table 1), its specific impact on the Da-An River gorge was documented by two RTK GPS surveys conducted before and after the wet season. The knickzone-long incision in summer, 2009 (Fig. 5C) was the result of the flood induced by Typhoon Morakot. We thus, conclude the number and the magnitude of large flooding events control the amount of bedrock incision and knickpoint migration. Our observations match previous geomorphic observations that rivers incise valleys only during the largest floods (e.g., Baker, 1977; Wolman and Gerson, 1978; Lamb and Fonstad, 2010). These floods not only transport sediments, especially bed load, but also expose the bedrock floor to processes such as abrasion and plucking (e.g., Pickup and Warner, 1976). Therefore, the rate of fluvial incision depends on the recurrence interval of these large and rare flooding events (Molnar et al., 2006).

Although the large flood events are keys in pushing the channel past the erosional threshold to initiate knickpoint migration, once this boundary is crossed, precipitation/discharge is no longer a first order control. The assumption is based on the

findings that no significant correlation was found between the amount of knickpoint migration and total precipitation (Fig. 12A), maximum daily precipitation (Fig. 12B), or maximum hourly precipitation (Fig. 12C).

## **5.2 Structural and Lithologic Controls on the Evolution of the Da-An River Gorge**

The morphology of the Da-An River gorge is strongly influenced by jointing. Along the incised reach of the Da-An River, the Pliocene Cholan Formation is characterized by a dominate set of joint planes striking from  $310^{\circ}$  to  $354^{\circ}$  (Fig. 7). This joint orientation matches the local flow direction of the Da-An River. It appears that the channel has exploited the steeply-dipping joint planes to incise via plucking (Hancock et al., 1998; Whipple et al., 2000a, 2000b). In addition, plucking and abrasion on the exposed bedrock channel floor drives the vertical lowering of the reach above knickpoints that reduce the height of the knickpoint face when migrating upstream. The jointing, therefore, not only controls the morphology of the bedrock channels but also the style of knickpoint migration.

The knickpoint development and upstream migration in the Da-An River reveals the strong influence bedrock geology and structure, which complements previous observations in south-central Indiana, USA (Miller et al., 1991) and Niagara Falls (Gilbert, 1907; Tinkler et al., 1994; Hayakawa and Matsukura, 2009; Lamb and Dietrich, 2009). The morphology of the knickpoints and the style of knickpoint retreat in the Da-An River gorge have been influenced by lithological variation and by changes in the dip of bedding across the anticline. We observed that individual knickpoints were developed on thick layers of resistant siltstone because the actual shear stress generated by the river flow on the surface of siltstone is too low to erode it during low-flow regimes (Figs. 8C and 8D). The knickpoints in the sequential longitudinal profiles show that their height depends on the locations in the anticline, in other words, the dip of bedrock bedding (Fig. 8A). In the western (downstream) limb of the anticline, the knickpoint developed on the

steep reaches formed after uplift (Fig. 5B); the heights of these knickpoints grew during wet seasons. A 3-m- to 4-m-high knickpoint was found after the 1999 earthquake. Six years later, two knickpoints with heights of 8 m and 13 m were recognized in the 2005 longitudinal profile (Fig. 5C). The knickpoints then built up as one with a height of 10 to 15 m in the hinge zone between the western limb and the flat top of the anticline in 2006. In the flat top of the anticline, knickpoints were developed on a resistant siltstone layer underlain by non-resistant mudstone strata with maximum height throughout the anticline. Here the knickpoint propagation was initiated by the removal of material from the plunge pool at the base of the knickpoints, where the non-resistant layers located (Gardner, 1983). The undermining of the relatively resistant siltstone caprock caused its collapse and retreat of the whole knickpoint face. The height of knickpoint remained constant in these processes (Figs. 5C and 8A). As the knickpoint migrated upstream through the eastern hinge zone, the knickpoint heights decreased in response to the changes in bedrock dips from horizontal to upstream-dipping (Figs. 5C and 8A). The knickpoint faces rotated as the result of upstream incision (Figs. 9C and 9D) and downstream aggradation (Figs. 9A and 9B) (Gardner, 1983). In the eastern limb of the Tungshih anticline, knickpoint retreat processes is a combination of vertical lowering of the bedrock channel bottoms and upstream migration of the knickpoint faces in the upstream-dipping bedrock (Figs. 5C and 8A). This knickpoint behavior, known as replacement, reduced the relief across the waterfall (Gardner, 1983; Frankel et al., 2007). Therefore, in the eastern limb and in the horizontal layers upstream from the anticline, the knickpoints were only 2 to 4 m high (Figs. 5C and 8D), which were approximately the thickness of the resistant substrate where they localized.

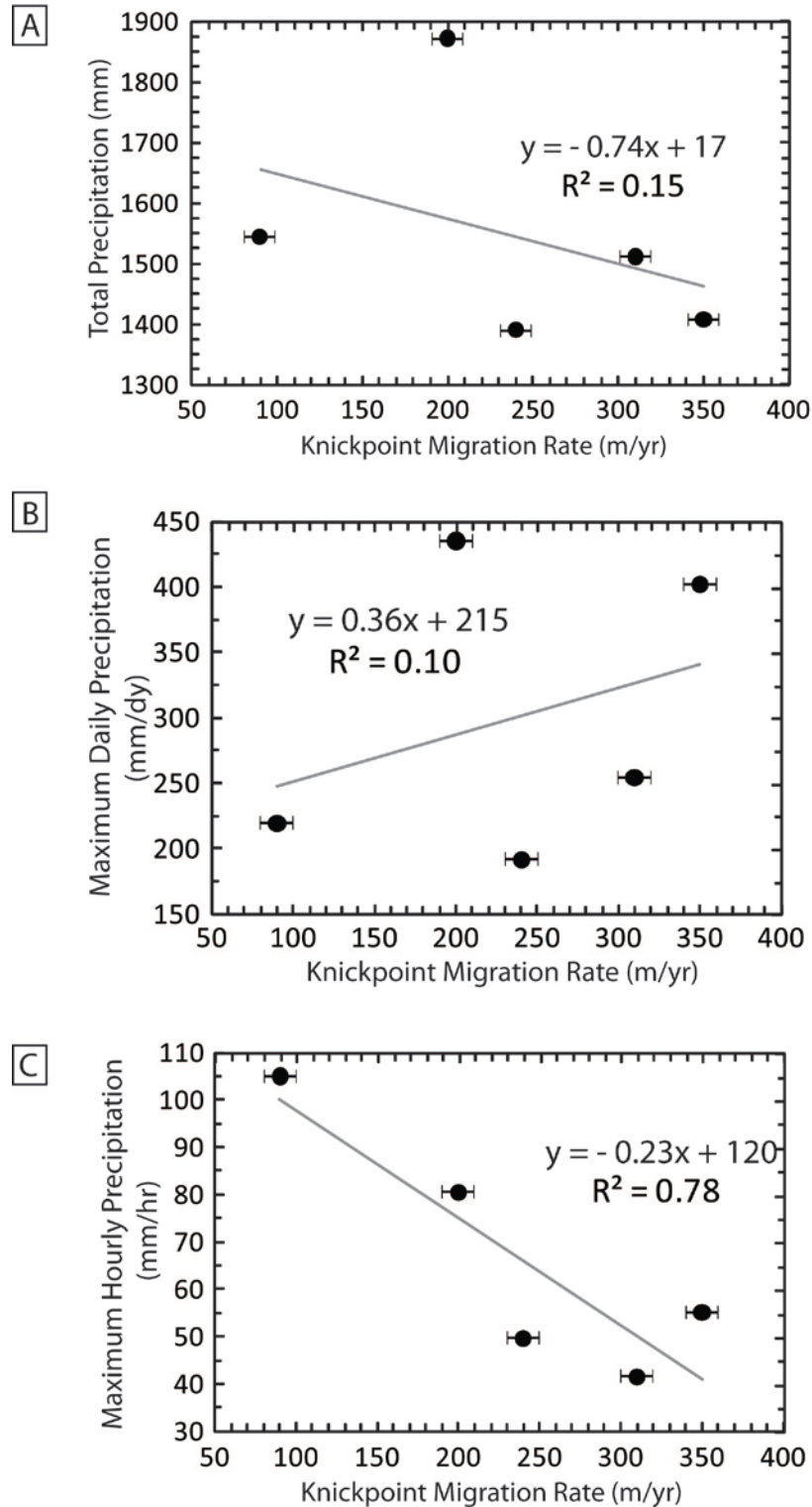


Figure 12. Linear regressions performed on knickpoint migration rate as a function of total precipitation (A), maximum daily precipitation (B), and maximum hourly precipitation (C) at the Cholan Station over the time period 2004 to 2009. Note that the uncertainties on precipitation are  $\pm 3\%$  of their values, the ranges smaller than the diameter of black dots in all cases. Thus the uncertainties of the precipitation values are not shown on the graphs.

Knickpoint retreat in the Da-An River gorge was unsteady in response to the variable dip of bedding across the Tungshih anticline (Fig. 4B). The rates of knickpoint retreat, once a discharge threshold is crossed, are affected by the dip of bedding (Table 2; Fig. 11). Because three different knickpoint models: parallel retreat, rotation, and replacement were observed in the flat top, hinge zone (between flap and eastern limb), and eastern limb, respectively (Fig. 8A), the knickpoint migration rates are correlated to the knickpoint evolution behaviors. The highest knickpoint migration rates ( $> 300$  m/yr) were recorded in flat-lying, horizontal strata ( $< 10^\circ$ ) in which a parallel retreat was the dominant process (Table 2; Fig. 8A). This rapid parallel retreat knickpoint migration occurred through a section of the strata where a several-meter-thick siltstone overlies thinly-bedded mudstone layers in the flat top of the Tungshih anticline. The underlying nonresistant substrate retreats relatively quickly and cap rock immediately follows by collapsing from the lip of knickpoint after the underlying substrate becomes undermined (Gardner, 1983). The erosion of resistant rock is driven by gravity and weathering processes, which are more efficient degradation processes than stream power, which generate shear stress less than actual shear stress on resistant rock (Gardner, 1983). On the contrary, the execution of rotation and replacement processes relies heavily on stream power. Moreover, both models involve vertical incision into resistant bedrock in the Da-An River gorge (Fig. 8A), thereby producing lower rates of knickpoint migration. Therefore, parallel retreat exhibits the fastest retreat rates than other knickpoint migration models (e.g., Philbrick, 1970, 1974; Gardner, 1983; Frankel et al., 2007).

### **5.3 Implications for River Response to Coseismic Uplift**

Based on temporal monitoring on the Da-An River in the first 10 years after the Chi-Chi earthquake, we propose a general conceptual model for the recovery of fluvial systems after base-level fall by active uplift and folding such as the Tungshih anticline and following incision in the downstream non-deformed reach. This model lends insight

to rapid erosional response of a river after essentially instantaneous uplift of an alluvium-covered reach. Our model shares some characteristics with the model for changes in ephemeral stream channel pattern and morphology responding to growing fold proposed by Pearce et al. (2004). The scheme begins with an alluvium-covered reach that orthogonally crosses the axis of an anticline with a uniform gradient (Fig. 13A). The instantaneous growth of the anticline in an earthquake uplifts a segment of the reach for several meters, which generates steep reaches on the fold limb facing downstream and gentler-than-pre-earthquake reaches on the fold limb facing upstream (Fig. 13B). Knickpoints are developed on these steep reaches as sharp contacts in lithology where the alluvium mantles are removed immediately after the earthquake by enhanced erosion (e.g., Miller et al., 1991) (Figs. 2B and 8A). Following coseismic uplift, climate enhances modification of the deformed landscape by various magnitudes of flooding, which accelerates the response process to base level fall.

Knickpoint retreat in downstream limbs initiates during low to moderate magnitude, higher frequency floods. Above knickpoint lips, reaches on the other limb of the anticline are lowered by vertical incision (Fig. 13C) as the result of the increase in flow velocity and shear stress at the waterfall lip (Haviv et al., 2006). In the flat top or the axis of the fold, the down-cutting process preserves strath terraces (Fig. 2C), which also have been observed in the reach where an ephemeral stream crosses an active fold axis (Pearce et al., 2004). The base level is lowered additionally as the result of flow acceleration, by which the non-deformed reach immediately downstream is incised into the bedrock. The channel bed is therefore below the pre-earthquake level after excess erosion. When the first rare large flood take place, it triggers upstream knickpoint retreat accompanied by excess erosion with the amount comparable to the coseismic uplift in the reach below the knickpoint toe and amplified erosion above the knickpoint lip (Fig. 13D). The knickpoints reach maximum height when arrive at the flat top of the anticline. Afterward, migration in upstream-dipping strata results in a decrease in knickpoint height

during each subsequent flood-induced upstream migration (Fig. 13E). Eventually, the incision signals and knickpoints, which facilitate new bedrock exposure, pass over the upstream limit of deformation zones and continue to migrate upstream, until touch the headwater area (Fig. 13F).

Incision of the channel is a hybrid process including vertical erosion through alluvium and upstream knickpoint migration in bedrock. The interaction of these processes is expressed as rotation, replacement, and parallel retreat behavior with respect to different bedding dips in anticlines. Ultimately, knickpoints reduce their height on the way to through the basin toward the drainage divide. Therefore, the overall style of knickpoint migration is close to replacement in which the rate of vertical incision upstream of the knickpoint face is equal to, or slightly faster than, rate of parallel retreat (Frankel et al., 2007). Because the erosion wave will attenuate as the knickpoint lip lowers in elevation as it moves upstream, the initial knickpoint height and rate of height decrease controls the distance of erosion signal traveled (Holland and Pickup, 1976). The response time of the fluvial system to tectonic forcing depends on knickpoint propagation rate and knickpoint decay rate. Our study shows a 1300 m of knickpoint retreat (Fig. 4B) and a 13 m-to-3m decrease in height for the major knickpoint (Fig. 5C) within the 10 years after the tectonic uplift.

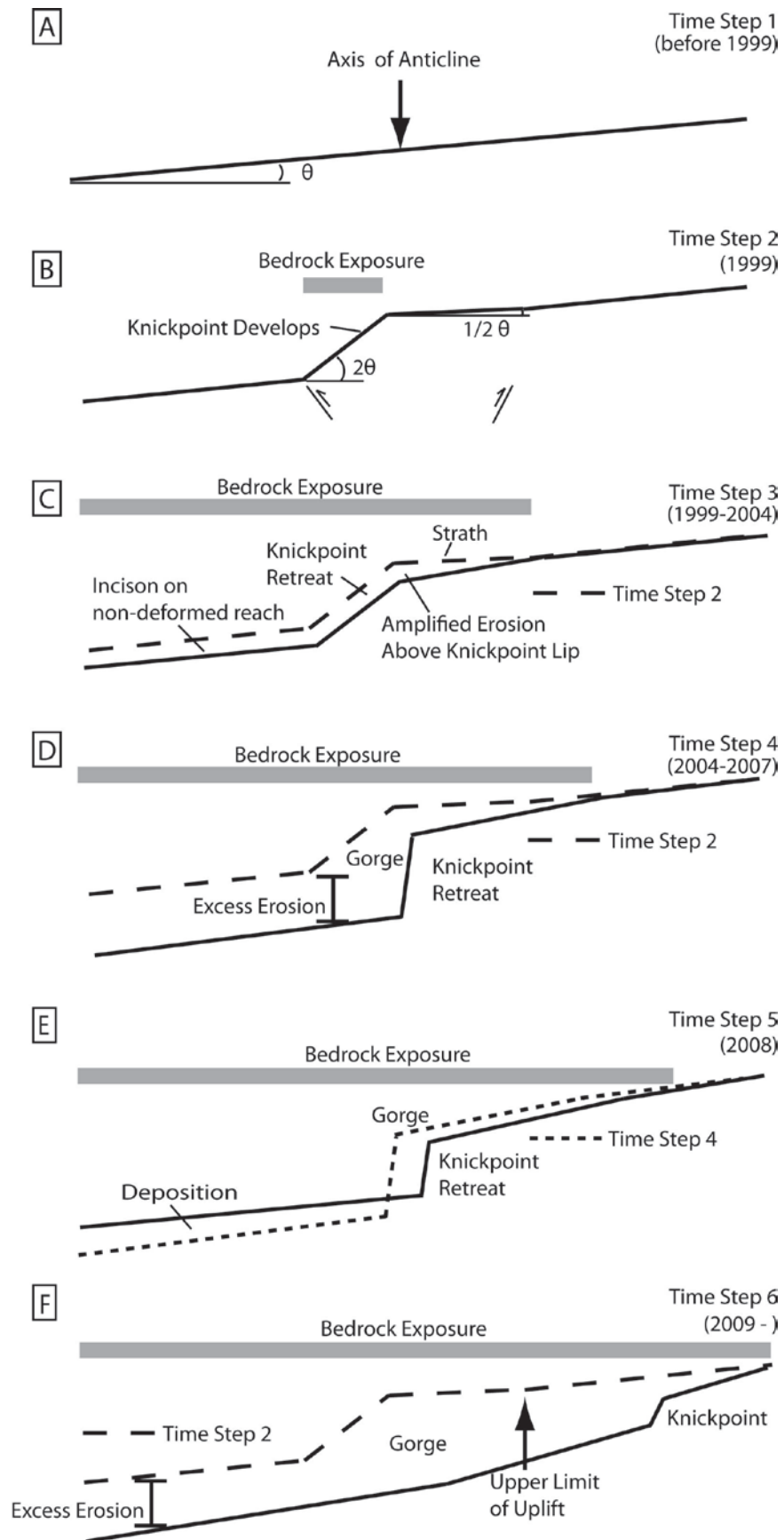




Figure 13. Schematic diagram delineating river response to coseismic uplift based on observations of the Da-An River in the 10 years following the 1999 Chi-Chi earthquake. (A) The scheme begins with an alluvium-covered reach which orthogonally crosses the axis of an anticline with a uniform gradient. (B) The instantaneous growth of the anticline in an earthquake uplifts a segment of the reach for several meters, which generates steep reaches on the fold limb facing downstream and gentler than pre-earthquake reaches on the fold limb facing upstream. The knickpoints are developed on these steep reaches as sharp contacts in lithology where the alluvium mantles are removed immediately after the earthquake by enhanced erosion. (C) Knickpoint retreat in downstream limbs initiates during low to moderate magnitude, higher frequency floods. Above knickpoint lips, reaches on the other limb of the anticline are lowered by vertical incision, which preserves strath terraces. The base level is lowered additionally as the result of flow acceleration, where the non-deformed reach immediately downstream is incised into the bedrock. (D) When the first rare large flood takes place, they trigger upstream knickpoint retreat accompanied by excess erosion with the amount comparable to the coseismic uplift in the reach below the knickpoint toe and amplified erosion above the knickpoint lip. The knickpoints reach maximum height in the flat top of the anticline. (E) The knickpoints migrate through upstream-dipping strata with significant amounts of sediments from the erosion of upstream reaches are deposited at the toes of the knickpoints, resulting in a decrease in knickpoint height during each subsequent flood-induced upstream migration. (F) The incision signals and knickpoints pass over the boundary of deformation zones and propagate throughout the entire basin.

## **CHAPTER 6**

### **CONCLUSIONS**

The evolution of the Da-An River gorge provides an excellent opportunity to study fluvial response to tectonic uplift. The complex channel response here reflects the interaction between tectonics, climate, lithology and structure. Tectonics doubled the channel gradient and lowered the base level of the reach during coseismic uplift in the Chi-Chi earthquake. Afterwards, climate triggered erosion in the uplifted reach and non-deformed reach immediately downstream in response to the changing boundary conditions. The bedrock incision in the non-deformed reach downstream further lowered the local base level that caused “excess” erosion in the Da-An River gorge, where the channel bed was significantly lower than the pre-uplifted channel.

Other than tectonics and climate, bedrock structure and lithology also showed the influence on the evolution of the Da-An River gorge. The morphology of the bedrock channels and the knickpoints is strongly influenced by jointing and bedding dip. In the knickzone, joint planes control the downcutting of channels and flow direction. The total knickpoint relief depends on the location in the Tungshih anticline with the highest knickpoints (10 to 15 m) developed in the flat top the anticline. The changes in the dip of the bedding across the anticline also control the rates and styles of knickpoint propagation. Parallel retreat was the most prominent style for knickpoint evolution in the horizontal beds and the strata dipping downstream, while replacement was observed in the strata dipping upstream. Rotation occurred in a hinge zone where the bedding dips change from horizontal to upstream-dipping. The maximum propagation rate (300 to 350 m/yr) occurred in the horizontal layers in which knickpoints migrate upstream through parallel retreat processes.

A conceptual model is presented to illustrate fluvial response to immediate

growing of active folds. The instantaneous growth of the anticline in an earthquake uplifts a segment of the river and generates steep reaches where knickpoints developed. Climate accelerates the responsive processes to base level falling by various magnitudes of flooding that induces knickpoint migration. The base level is lowered additionally by the bedrock incision the non-deformed reach immediately downstream that causes the channel bed below the pre-earthquake level. Eventually, the incision signals and knickpoints, which facilitate new bedrock exposure, pass over the boundary of deformation zones and continue to migrate upstream, until the headwater area where decaying knickpoints lose their height. The response time of fluvial system is defined by how fast knickpoints migrate upstream, which is controlled by frequency and magnitude of floods and dip of bedrock. However, further numerical or analytical investigations are needed to quantify their influence on landscape erosion to short-term rock uplift.

## **APPENDIX A**

### **FIELD SURVEY METHODOLOGY AND UNCERTAINTIES**

The RTK GPS system involves two GPS units, including two Leica GX1230+ GPS dual frequency RTK receivers equipped with two Leica AX1202 Dual Frequency GPS/GLONASS Antennas, kept in contact by two Pacific Crest PDL radios. One GPS unit was set up as the fixed base station, while the other as the mobile rover. The survey points were measured by the rover unit after differentiating the position relative to the base station. This technique significantly canceled out most of the errors inherent in a single GPS system by solving the local baselines thus the uncertainties of the rover unit positions were reduced from 2-3 m (when working independently) to 0.01-0.02 m in 3-D. Because we compared the sequential channel change of the Da-An River, every survey results were tied to a continuous GPS station, the Penghu station (S01R) in the Taiwan Strait for a fixed reference frame. For the reach could not be reached safely, we used a laser rangefinder, Contour XLRic from LaserCraft Inc., to measure the distance from the shooting points, which have RTK GPS coordinates, to our targets.

The uncertainties of xyz coordinates measured from the RTK GPS, at a 95% confidence level, are of 10 mm + 1 ppm of the signal RMS in the horizontals, and of 20 mm + 1 ppm in the verticals. Because all rover measurements were taken within the distance of 4 km from the base station, our RTK GPS points have the uncertainties of 14 mm in horizontal directions and 24 mm in vertical directions. The uncertainty of the laser rangefinder measurement is 150 mm for the object 80 m away. Thus for the inaccessible places, where the distance between the RTK coordinates and the inaccessible places was measured from the laser rangefinder, errors associated with the laser were added to those related to the RTK GPS measurement of the position of the shooting point. Because we never shoot water levels from a distance of more than 80 m, the xyz coordinates of the points

measured by the combination of the RTK GPS system and the laser rangefinder have an uncertainty of 200 mm in 3-D.

## REFERENCES

- Amos, C.B., and Burbank D.W., 2007, Channel width response to differential uplift: *Journal of Geophysical Research*, v. 112, F02010, doi: 10.1029/2006JF000672.
- Attal, M., Tucker, G.E., Whittaker, A.C., and Cowie, P.A., and Roberts, G.P., 2008, Modeling fluvial incision and transient landscape evolution: Influence of dynamic channel adjustment: *Journal of Geophysical Research*, v. 113, F03S06, doi: 10.1029/2007JF000893.
- Baker, V.R., 1977, Stream-channel response to floods, with example from central Texas: *Geological Society of America Bulletin*, v. 88, p. 1057–1071.
- Berlin, M.M., and Anderson, R.S., 2007, Modeling of knickpoint retreat on the Roan Plateau, western Colorado: *Journal of Geophysical Research*, v. 112, F03S06, doi: 10.1029/2006JF000553
- Brummer, C.J., and Montgomery, D.R., 2006, Influence of coarse lag formation on the mechanics of sediment pulse dispersion in a mountain stream, Squire Creek, North Cascades, Washington, United States: *Water Resources Research*, v. 42, W07412, doi: 10.1029/2005WR004776.
- Bull, W.B., 1979, Threshold of critical power in streams: *Geological Society of America Bulletin*, v. 90, p. 453–464.
- Central Geological Survey, 1999, Investigation report of the 921 earthquake geology and map of surface ruptures along the Chelungpu fault during the 1999 Chi-Chi earthquake: Taiwan, Ministry of Economic Affairs (in Chinese).
- Chang, C.H., Wu, Y.M., Shin, T.C., and Wang, C.Y., 2000, Relocation of the 1999 Chi-Chi earthquake in Taiwan: *Terrestrial, Atmospheric, and Oceanic Sciences*, v. 11, p. 581–590.
- Chen, W.S., Lee, K.J., Lee, L.S., Ponti, D.J., Prentice, C., Chen, Y.G., Chang, H.C., and Lee, Y.H., 2004, Paleoseismology of the Chelungpu fault during the past 1900 years: *Quaternary International*, v. 115, p. 167–176.
- Chen, Y.G., Lai, K.Y., Lee, Y.H., Suppe, J., Chen, W.S., Lin, Y.N.N., Wang, Y., Hung, J.H., and Kuo, Y.T., 2007, Coseismic fold scarps and their kinematic behavior in the 1999 Chi-Chi earthquake Taiwan: *Journal of Geophysical Research*, v. 112, B03S02, doi: 10.1029/2006JB004388.

- Clark, M.K., Schoenbohm, L.M., Royden, L.H., Whipple, K.X., Burchfiel, B.C., Zhang, X., Tang, W., Wang, E., and Chen, L., 2004, Surface uplift, tectonics, and erosion of eastern Tibet from large-scale drainage patterns: *Tectonics*, v. 23, TC1006, doi: 10.1029/2002TC001402.
- Craddock, W.H., Burbank, D.W., Bookhagen, B., and Gabet, E.J., 2007., Bedrock channel geometry along an orographic rainfall gradient in the upper Maryandi River valley in central Nepal: *Journal of Geophysical Research*, v. 112, F03007, doi: 10.1029/2006JF000589.
- Crosby, B.T., and Whipple, K.X., 2006, Knickpoint initiation and distribution within fluvial networks: 236 waterfalls in the Waipaoa River, North Island, New Zealand: *Geomorphology*, v. 82, p.16–38.
- Dadson, S.J., Hovius, N., Chen, H., Dada, W.B., Hsieh, M.L., Willett, S.D., Hu, J.C., Horng, M.J., Chen, M.C., Stark, C.P., Lague, D., and Lin, J.C., 2003, Links between erosion, runoff variability and seismicity in the Taiwan orogen: *Nature*, v. 426, p. 648–651.
- Dadson, S.J., Hovius, N., Pegg, S., Dade, W.B., Horng, M.J., and Chen, H., 2005, Hyperpycnal river flows from an active mountain belt: *Journal of Geophysical Research*, v. 110, F01016, doi: 10.1029/2004JF000244.
- Douglass, J., and Schmeeckle, M., 2007, Analog modeling of transverse drainage mechanisms: *Geomorphology*, v. 84, p. 22–43.
- Duvall, A., Kirby, E., and Burbank, W., 2004, Tectonic and lithologic controls on bedrock channel profiles and processes in coastal California: *Journal of Geophysical Research*, v. 109, F03002, doi: 10.1029/2003JF000086.
- Frankel, K.L., Pazzaglia, F.J., and Vaughn, J.D., 2007, Knickpoint evolution in a vertically bedded substrate, upstream dipping terraces, and Atlantic slope bedrock channels: *Geological Society of America Bulletin*, v. 119, p. 476–486, doi: 10.1130/B25965.1.
- Finnegan, N.J., Sklar, L.S., and Fuller, T.K., 2007, Interplay of sediment supply, river incision, and channel morphology revealed by the transient evolution of an experimental bedrock channel: *Journal of Geophysical Research*, v. 112, F03S11, doi: 10.1029/2006JF000569.
- Finnegan, N.J., Roe, G., Montgomery, D.R., Hallet, B., 2005, Controls on the channel width of rivers: Implications for modeling fluvial incision of bedrock: *Geology*, v. 33, p. 229–232.

- Gardner, T.W., 1983, Experimental study of knickpoint and longitudinal profile evolution in cohesive, homogeneous materials: *Geological Society of America Bulletin*, v. 94, p. 664–672.
- Gilbert, G.K., 1907, Rate of recession of Niagara Falls: *U.S. Geological Survey Bulletin*, v. 306, 31 p.
- Gran, K.B., and Montgomery, D.R., 2005, Spatial and temporal patterns in fluvial recovery following volcanic eruptions: channel response to basin-wide sediment loading at Mount Pinatubo, Philippines: *Geological Society of America Bulletin*, v. 117, p. 195–211.
- Hack, J.T., 1960, Interpretation of erosional topography in humid temperate regions: *American Journal of Sciences*, v. 258-A, p. 80–97.
- Hancock, G.S., Anderson, R.S., and Whipple, K.X., 1998, Beyond power: Bedrock river incision processes and form, *in* Tinkler, K.J., and Wohl, E.E., eds., *Rivers over Rock: Fluvial Processes in Bedrock Channels*: American Geophysical Union Geophysical Monograph 107, p. 35–60.
- Harkins, N., Kirby, E., Heimsath, A., Robinson, R., and Reiser, U., 2007, Transient fluvial incision in the headwaters of the Yellow River, northeastern Tibet, China: *Journal of Geophysical Research*, v. 112, F03S04, doi: 10.1029/2006JF000570.
- Haviv, I., Enzel, Y., Whipple, K.X., Zilberman, E., Stone, J., Matmon, A., and Fifield, L.K., 2006, Amplified erosion above waterfalls and oversteepened bedrock reaches: *Journal of Geophysical Research*, v. 111, F04004, doi: 10.1029/2006JF000461.
- Hayakawa, Y., and Matsukura, Y., 2009, Factors influencing the recession rate of Niagara Falls since the 19th century: *Geomorphology*, v. 110, p. 212–216.
- Ho, C.S., 1982. Tectonic evolution of Taiwan: Explanatory text of the tectonic map of Taiwan: Taipei, Ministry of Economic Affairs (in Chinese).
- Holland, W.N., and Pickup, G., 1976, Flume study of knickpoint development in stratified sediment: *Geological Society of America Bulletin*, v. 87. p. 76–82.
- Howard, A.D., 1994, A detachment-limited model of drainage basin evolution: *Water Resource Research*, v. 30, p. 2261–2285.
- Hu, C.C., and Chiu, C.T., 1984, Deep structures of the Cholan Area, Northern Taiwan: *Petroleum Geology of Taiwan*, v. 20, p.21–33.
- Hydrological Yearbook of Taiwan, R. O. C., 1904-2008: Taipei, Taiwan, Water Resources Bureau.



- Institute of Earth Sciences, 1999, Institute of Earth Science The Chi-Chi Earthquake in Taiwan: [http://www.earth.sinica.edu.tw/921/921chichi\\_main\\_eng.htm](http://www.earth.sinica.edu.tw/921/921chichi_main_eng.htm).
- Johnson, J.P.L., and Whipple, K.X., 2007, Feedbacks between erosion and sediment transport in experimental bedrock channels: *Earth Surface Processes and Landforms*, v. 32, p.1048–1062.
- Johnson, J.P.L., Whipple, K.X., Sklar, L.S., and Hanks, T.C., 2009, Transport slopes, sediment cover, and bedrock channel incision in the Henry Mountains, Utah: *Journal of Geophysical Research*, v. 114, F02014, doi: 10.1029/2007JF000862.
- Kao, H., and Chen, W.P., 2000, The Chi-Chi earthquake sequence: active out-of-sequence thrust faulting in Taiwan: *Science*, v. 288, p. 2346–2349.
- Kirby, E., Johnson, C., Furlong, K., Hesath, A., 2007, Transient channel incision along Bolinas Ridge, California: Evidence for differential rock uplift adjacent to the San Andreas fault: *Journal of Geophysical Research*, v. 112, F03S07, doi: 10.1029/2006JF000559
- Lamb, M.P., and Dietrich, W.E., 2009, The persistence of waterfalls in fractured rock: *Geological Society of America Bulletin*, v. 121, p. 1123–1134.
- Lamb, M.P., and Fonstad, M.A., 2010, Rapid formation of a modern bedrock canyon by a single flood event: *Nature Geoscience*, v. 2, p. 477–481.
- Lavé, J., and Avouac, J.P., 2001, Fluvial incision and tectonic uplift across the Himalayas of central Nepal: *Journal of Geophysical Research*, v. 106, p. 26,561–26,591.
- Lee, J.C., Chu, H.T., Angelier, J., Chan, Y.C., Hu, J.C., Lu, C.Y., and Rau, R.J., 2002, Geometry and structure of northern surface ruptures of the 1999 Mw=7.6 Chi-Chi, Taiwan earthquake: Influence from inherited fold belt structures: *Journal of Structural Geology*, v. 24, p. 173–192.
- Lee, Y.H., Lu, S.T., Shih, T.S., Hsieh, M.L., and Wu, W.Y., 2005, Structures associated with the northern end of the 1999 Chi-Chi earthquake rupture, central Taiwan: Implications for seismic-hazard assessment: *Bulletin of Seismological Society of America*, v. 95, p. 471–485.
- Leopold, L.B., and Maddock, T., 1953, The hydraulic geometry of stream channels and some physiographic implications, U.S. Geological Survey Professional Paper 252.
- Ma, K.F., Lee, C.T., and Tsai, Y.B., 1999, The Chi-Chi, Taiwan, earthquake: large surface displacements on an inland fault: *Eos (Transactions, American Geophysical Union)*, v. 80, p. 605–611.

- Meng, C.Y., 1963, San-I overthrust: *Petroleum Geology of Taiwan*, v. 2, p. 1–20.
- Merritts D., and Vincent, K.R., 1989, Geomorphic response of coastal streams to low, intermediate, and high rates of uplift, Mendocino junction region, northern California: *Geological Society of America Bulletin*, v. 101, p.1373–1388, doi: 10.1130/0016-7606(1989)101<1373:GROCST>2.3.CO;2.
- Miller, J.R., 1991, The influence of bedrock geology on knickpoint development and channel-bed degradation along downcutting streams in south-central Indiana: *The Journal of Geology*, v. 99, p. 591–605.
- Molnar, P., Anderson, R.S., Kier, G., and Rose, J., 2006, Relationships among probability distributions of stream discharges in floods, climate, bed load transport, and river incision: *Journal of Geophysical Research*, v.111, F02001, doi: 10.1029/2005JF000310.
- Oskin, M., and Burbank, D.W., 2007, Transient landscape evolution of basement-cored uplifts: example of the Kyrgyz Range, Tian Shan: *Journal of Geophysical Research*, v. 112, F03S03, doi: 10.1029/2006JF000563.
- Ouimet, W., Whipple, K.X., Royden, L.H., Sun, Z., and Chen, Z., 2007, The Influence of Large Landslides on River Incision in a Transient Landscape: Eastern Margin of the Tibetan Plateau (Sichuan , China): *Geological Society of America Bulletin*, v. 119, p. 1462-1476, doi: 10.1130/B26136.1.
- Parker, G., Muto, T., Akamatsu, Y., Dietrich, W.E., and Lauer, J.W., 2008a, Unravelling the conundrum of river response to rising sea-level from laboratory to field. Part I: Laboratory experiments: *Sedimentology*, v. 55, p. 1643–1655.
- Parker, G., Muto, T., Akamatsu, Y., Dietrich, W.E., and Lauer, J.W., 2008b, Unravelling the conundrum of river response to rising sea-level from laboratory to field. Part II: The Fly-Stickland River system, Papua New Guinea: *Sedimentology*, v. 55, p. 1657–1686.
- Pearce, S.A., Pazzaglia, F.J., and Eppes, M.C., 2004, Ephemeral stream response to growing folds: *Geological Society of America Bulletin*, v. 116, p. 1223–1239. doi: 10.1130/B5386.1.
- Pelletier, J.D., 2009, The impact of snowbelt on the late Cenozoic landscape of the southern Rocky Mountain, USA: *GSA Today*, v. 19, doi: 10.1130/GSATG44A.1.
- Philbrick, S.S., 1970, Horizontal configuration and the rate erosion of Niagara Falls: *Geological Society of America Bulletin*, v. 81, p. 3723–3732.
- Philbrick, S.S., 1974, What future for Niagara Falls?: *Geological Society of America Bulletin*, v. 85, p. 91–98.

- Pickup, G., and Warner, R.F., 1976, Effects of hydrologic regimes on the magnitude and frequency of dominate floods: *Journal of Hydrology*, v. 158, p. 219–240.
- Reusser, L.J., Bierman, P.R., Pavich, M.J., Zen, E., Larson, J., and Finkel, R., 2004, Rapid late Pleistocene incision of Atlantic passive margin river gorges: *Science*, v. 305, p. 499–502.
- Schildgen, T.F., Balco, G., and Shuster, D.L., 2010, Canyon incision and knickpoint propagation recorded by apatite  $^4\text{He}/^3\text{He}$  thermochronometry: *Earth and Planetary Science Letters*, v. 293, p. 377–387.
- Shin, T.C., 2000, Some seismological aspects of the 1999 Chi-Chi earthquake in Taiwan: *Terrestrial, Atmospheric, and Oceanic Sciences*, v. 11, p. 555–566.
- Sklar, L.S., Stock, J.D., Roering, J.J., Chi, W.C., Kirchner, J.W., Dietrich, W.E., Hsu, L., Hsieh, M.L., Tsao, S.J., and Chen, M.M., 2005, Evolution of fault scarp knickpoints following September 1999 Chi-Chi earthquake in West-Central Taiwan: *Eos (Transactions, American Geophysical Union)*, v. 86, Fall meeting supplement, abstract H34A-06.
- Snyder, N.P., Whipple, K.X., Tucker, G.E., and Merritts, D.J., 2003, Channel response to tectonic forcing: field analysis of stream morphology and hydrology in the Mendocino triple junction region, northern California: *Geomorphology*, v. 53, p. 97–190.
- Stark, C.P., 2006, A self-regulating model of bedrock river channel geometry: *Geophysical Research Letters*, v. 33, L04402, doi: 10.1029/2005GL023193.
- Stein, O.R., and Julien, P.Y., 1993, Criterion delineating the mode of headcut migration: *Journal of Hydraulic Engineering*, v. 119, p. 37-50.
- Stock, G.M., Anderson, R.S., and Finkel, R.C., 2004, Pace of landscape evolution in the Sierra Nevada, California, revealed by cosmogenic dating of cave sediments: *Geology*, v.32, p.193–196.
- Stock, J.D., Montgomery, D.R., Collins, B.D., Dietrich, W.E., Sklar, L.S., 2005, Implications for process controls on the long profiles of valley cut by river and debris flows: *Geological Society of America Bulletin*, v. 117, p. 174–194.
- Tinkler, K.J., and Wohl, E.E., 1998, *Rivers over rock: Fluvial Processes in Bedrock Channels*: American Geophysical Union Geophysical Monograph 107, Washington, D.C.

- Tinkler, K.J., Pengelly, J.W., Asselin, G., and Parkins, W.G., 1994, Postglacial recession of Niagara Falls in relation to the Great Lakes: *Quaternary Research*, v. 42, p. 20–29. Washington, D.C.
- Turowski, J.M., Lague, D., and Hovius, N., 2009, Response of bedrock channel width to tectonic forcing: Insights from a numerical model, theoretical considerations, and comparison with field data: *Journal of Geophysical Research*, v. 114, F03016, doi: 10.1029/2008JF001133
- Turowski, J.M., Lague, D., Crave, A., and Hovius, N., 2006, Experimental channel response to tectonic uplift: *Journal of Geophysical Research*, v. 111, F03008, doi: 10.1029/2005JF000306.
- Whipple, K.X., 2001, Fluvial landscape response time: How plausible is steady-state denudation?: *American Journal of Sciences*, v. 301, p. 313–325.
- Whipple, K.X., 2004, Bedrock rivers and geomorphology of active orogens: *Annual Review of Earth and Planetary Sciences*, v. 32, p.151–185.
- Whipple, K.X., and Tucker, G.E., 1999, Dynamics of the stream-power river incision model: Implications for height limits of mountain ranges, landscape response timescales, and research needs: *Journal of Geophysical Research*, v. 104, p. 17,661–17,674.
- Whipple, K.X., and Tucker, G.E., 2002, Implications of sediment-flux-dependent river incision models for landscape evolution: *Journal of Geophysical Research*, v. 107, doi: 10.1029/2000JB000044.
- Whipple, K.X., Hancock, G.S., and Anderson, R.S., 2000a, River incision into bedrock: Mechanics and relative efficacy of plucking, abrasion, and cavitation: *Geological Society of America Bulletin*, v. 112, p. 490–503.
- Whipple, K.X., Snyder, N.P., and Dollenmayer K., 2000b, Rates and processes of bedrock incision by the Upper Ukak River since the 1912 Novarupta ash flow in the Valley of Ten Thousand Smokes, Alaska: *Geology*, v. 28, p. 835–838.
- Whittaker, A.C., Cowie, P.A., Attal, M., Tucker, G.E., and Roberts, G.P., 2007a, Bedrock channel adjustment to tectonic forcing: Implications for predicting river incision rules: *Geology*, v. 35, p. 103–106.
- Whittaker, A.C., Cowie, A.C., Attal, M., Tucker, G.E., and Roberts, G.P., 2007b, Contrasting transient and steady-state rivers crossing active normal faults: new field observations from the Central Apennines, Italy: *Basin Research*, v. 19, p. 529–556.

- Wobus, C.W., Kean, J.W., Tucker, G.E., and Anderson, R.S., 2008, Modeling the evolution of channel shape: Balancing computational efficiency with hydraulic fidelity: *Journal of Geophysical Research*, v. 113, F02004, doi: 10.1029/2007JF000914.
- Wolman, M.G., and Gerson, R., 1978, Relative scales of time and effectiveness of climate in watershed geomorphology: *Earth Surface Processes and Landforms*, v. 3, p. 189–208.
- Yanites, B.J., Tucker, G.E., Mueller, K.J., Chen, Y.G., 2010a, How rivers react to large earthquakes: Evidence from central Taiwan: *Geology*, v. 38, p. 639–642.
- Yanites, B.J., Tucker, G.E., Mueller, K.J., Chen, Y.G., Wilcox, T., Huang, S.Y., and Shi, K.W., 2010b, Incision and channel morphology across active structures along the Peikang River, central Taiwan: Implications for the importance of channel width: *Geological Society of America Bulletin*, v. 122, p. 1192–1208.